

Journal of the Mississippi Academy of Sciences

Volume 62

July 2017

Number 3



Editor

Michelle Tucci
University of Mississippi Medical Center

Associate Editors

Hamed Benghuzzi
University of Mississippi Medical Center

Kenneth Butler
University of Mississippi Medical Center

Editorial Board

Gregorio Begonia
Jackson State University

Maria Begonia
Jackson State University

Ibrahim O. Farah
Jackson State University

Robin Rockhold
University of Mississippi Medical Center

Program Editors

Michelle Tucci
University of Mississippi Medical Center

Kenneth Butler
University of Mississippi Medical Center

Research Articles

- 308 **THE CIVIL WAR'S DEMOGRAPHIC IMPACT ON WHITE MALES IN MISSISSIPPI**
David A. Swanson and Richard Verdugo
- 316 **EVALUATION OF DROUGHT TOLERANT MAIZE GERMPLASM TO INDUCED DROUGHT STRESS**
Chathurika Wijewardana, W. Brien Henry, and K. Raja Reddy
- 330 **LOAD TRANSFER MECHANISMS OF BIOSTRUCTURES: A COMPLEX NETWORK APPROACH**
Reena R. Patel, Guillermo A. Riveros, David S. Thompson
- 334 **A STUDY OF LARGE-SCALE SURFACE FLUXES, PROCESSES AND HEAVY PRECIPITATION ASSOCIATED WITH LAND FALLING TROPICAL STORM LEE OVER GULF OF MEXICO USING REMOTE SENSING AND SATELLITE DATA**
Warith Abdullah, Remata Reddy, Ezat Heydari and Wilbur Walters Jackson

Departments

- 341 Call for Abstracts
- 342 MAS 2016 Membership and Meeting Information
- 343 Instructions for Abstracts and Poster Presentations
- 344 Author Information

The Journal of the Mississippi Academy of Sciences (ISSN 0076-9436) is published in January (annual meeting abstracts), April, July, and October, by the Mississippi Academy of Sciences. Members of the Academy receive the journal as part of their regular (nonstudent) membership. Inquiries regarding subscriptions, availability of back issues, and address changes should be addressed to The Mississippi Academy of Sciences, Post Office Box 55709, Jackson, MS 39296-5709, telephone 601-977-0627, or email msacademyofscience@comcast.net.

The Civil War's Demographic Impact on White Males in Mississippi

David A. Swanson¹ and Richard Verdugo²

¹University of California Riverside and ²National Education Association

Corresponding Author: David A. Swanson, Email: dswanson@ucr.edu

Richard Verdugo (retired), swamis65@yahoo.com

ABSTRACT

This paper provides an estimate of the demographic impact of the Civil War on white males in Mississippi. Our approach takes into account not only mortality, but also fertility and migration. It applies an impact analysis approach using 1850, 1860, and 1870 census counts of Mississippi. Cohort change ratios are constructed for ten-year age groups from the 1850 and 1860 census data and applied to the 1860 census data to project an expected number of white males by 10-year age groups for 1870. The demographic impact of the Civil War is estimated by subtracting the 1870 expected numbers by age from the 1870 census numbers by age, respectively. The analysis suggests that the war reduced the expected total number of white males by more than 12 percent. Substantial reductions are found to those who were of military age during the war, ranging from nearly 28 percent for those aged 30-39 in 1870 to nearly 17 percent for those aged 20-29 in 1870. The results are discussed and recommendations are provided, as well as descriptions of the data and methods

INTRODUCTION

Although there are exceptions (Holmes and Vinovskis 1992, Neely 2007), the usual approach to estimating the demographic impact of the Civil War is to examine mortality among soldiers (Faust 2006, Hacker 2011, Vinovskis 1989). In this paper, we take a broader perspective by estimating the full demographic impact of the Civil War on a population, rather than confining our interest to the war's mortality effects. This means we take into account the complete set of demographic components of change: fertility, mortality, and migration.

Conceptually, the approach we are taking was used by Swanson (2008) and Swanson et al. (2009) to assess the demographic impact of Hurricane Katrina on the Mississippi gulf coast and New Orleans, respectively. To illustrate this approach in regard to the impact of the Civil War we use the white male population of Mississippi as an example. This population is of interest because it largely provided the troops from Mississippi for the Confederate army, which means it likely suffered the largest demographic impacts in terms not only of mortality, but also in births and migration between 1860 and 1870.

Explained in detail in the following section, the approach we take involves projecting the pre-Civil War population to 1870 and comparing the "expected" results from the projection to the "actual" results as found in the 1870 census. For our example population, we make these comparisons across age groups. The projection method we employ encompasses all three of the demographic components of

change, fertility, mortality, and migration. It is known as the "Cohort Change Ratio Method" (Swanson 2008, Swanson and Tayman, 2012, Swanson et al. 2009, Swanson Tedrow and Baker forthcoming). However, as discussed later, it does not reveal the demographic impacts due to each component; instead it provides an estimate of their combined impacts. We later cover the strengths and weaknesses of this approach in the Discussion section.

DATA AND METHODS

The data used in this study were taken from 1850, 1860, and 1870 census counts of the U.S made available by the US Census Bureau (no date).

Table 1 provides the data used in this study. The 1850 and 1860 data are used to form cohort change ratios (CCRs), which are then applied to the 1860 data to affect a projection to 1870. See text for data sources.

AGE	1850	1860	1870
0-9	50,913	55,945	54,754
10-19	36,952	44,490	50,409
20-29	27,164	32,911	32,961
30-39	19,001	21,380	18,677
40-49	11,378	14,375	13,060
50-59	6,607	8,820	9,165
60+	4,045	5,622	7,818
TOTAL	156,060	183,543	186,844

Before describing the CCR method, it is useful to recall that any quantitative approach to forecasting is constrained to satisfy various mathematical identities (Land 1986). In regard to population forecasting, an approach should ideally satisfy demographic accounting identities, which is summarized in the fundamental demographic equation:

$$P_t = P_0 + B - D + I - O \quad [1]$$

That is, the population at some time in the future, P_t , must be equal to the population at an earlier time, P_0 , plus the births (B) and in-migrants (I) and less the deaths (D) and out-migrants (O) that occur between time 0 and time t . The most commonly used approach to population forecasting, cohort-component method, satisfies the fundamental equation, but it is data-intensive (George et al. 2004, Smith Tayman and Swanson 2013, Swanson and Tayman 2012: 201) and the data from the Civil War period are insufficient to support it.

As we show at the end of this section, the CCR Method also satisfies the fundamental demographic equation. However, it has far less intensive input data requirements than does the cohort-component method. Instead of mortality, fertility, migration, and total population data, which are required by the full-blown cohort-component method, the CCR method requires data only from the two most recent censuses (Hamilton and Perry 1962, Smith Tayman, and Swanson 2013: 176-181, Swanson, 2008, Swanson et al. 2009, Swanson Schlottmann, and Schmidt 2010, Swanson and Tayman 2012: 201-205, Swanson and Tedrow 2012).

The CCR method moves a population by age (and sex) from time t to time $t+k$ using cohort-change ratios (CCR) computed from data in the two most recent censuses. It consists of two steps. The first uses existing data to develop CCRs and the second applies the CCRs to the cohorts of the launch year population to move them into the future. As shown by Swanson, Schlottmann, and Schmidt (2010), the formula for developing a CCR is:

$${}_nCCR_{x,i,t} = \frac{{}_nP_{x,i,t}}{{}_nP_{x-k,i,t-k}} \quad [2]$$

where,

${}_nP_{x,i,t}$ is the population aged x to $x+n$ in area i at the most recent census (t),

${}_nP_{x-k,i,t-k}$ is the population aged $x-k$ to $x-k+n$ in area i at the

2nd most recent census ($t-k$), and

k is the number of years between the most recent census at time t and the one preceding it at time $t-k$.

The basic formula for the second step, moving the cohorts of a population into the future is:

$${}_nP_{x+k,i,t+k} = {}_nCCR_{x,i,t} \times {}_nP_{x,i,t} \quad [3]$$

where,

${}_nP_{x+k,i,t+k}$ is the population aged $x+k$ to $x+k+n$ in area i at time $t+k$, and

${}_nCCR_{x,i,t}$ and ${}_nP_{x,i,t}$ are as defined in equation [2].

Given the nature of the CCRs, 10-14 is the youngest five-year age group for which projections can be made if there are 10 years between censuses. To project the population aged 0-4 and 5-9 one can use the Child Woman Ratio (CWR) or more generally a “Child Adult Ratio” (CAR). These ratios do not require any data beyond what is available in the decennial census. For projecting the population aged 0-4, the CAR is defined as the population aged 0-4 divided by the population aged 20-34. For projecting the population aged 5-9, the CAR is defined as the population aged 5-9 divided by the population aged 25-39.

The CAR equations for projecting the population aged 0-4 and 5-9 are:

Population 0-4:

$${}_5P_{0,t+k} = ({}_5P_{0,t} / {}_{15}P_{20,t}) \times {}_{15}P_{20,t+k} \quad [4a]$$

Population 5-9:

$${}_5P_{5,t+k} = ({}_5P_{5,t} / {}_{15}P_{25,t}) \times {}_{15}P_{25,t+k} \quad [4b]$$

where

P is the population,

t is the year of the most recent census, and

$t+k$ is the projection year.

There are other “adult” age groups that could be used to define CAR (Smith, Tayman, and Swanson 2001: 156-157). The definitions shown in the two preceding equations are designed for a population in which fertility is at or below replacement, (i.e., the TFR is less than 2.1 or so), which correlates with the fact that first births tend to be postponed.

Another way to project the youngest age groups is to take their ratios at two points in time and apply that ratio to the launch year age group (t). In the first step, the ratios are as follows:

Population 0-4:

$${}_5R_{0,t} = {}_5P_{0,t} / {}_5P_{0,t-k} \quad [5a]$$

Population 5-9:

$${}_5R_{5,t} = {}_5P_{5,t} / {}_5P_{5,t-k} \quad [5b]$$

In the second step, the projected population at $t+k$ is found as follows:

Population 0-4:

$${}_5P_{0,t+k} = {}_5P_{0,t} \times {}_5R_{0,t} \quad [6a]$$

Population 5-9:

$${}_5P_{5,t+k} = {}_5P_{5,t} \times {}_5R_{5,t} \quad [6b]$$

We use the CAR method in this paper since it is better suited for our purposes, which is the projection of Mississippi white males by age from 1860 to 1870. One reason that it is better suited is that the CAR values are potentially affected by the impact of the Civil War whereas the ratios potentially would not be. Specifically, we use the ratio of those aged 0-9 to those aged 10 to 29.

Projections of the oldest open-ended age group also differ slightly from the projections for the age groups beyond age 10 up to the oldest open-ended age group. If for example the final closed age group is 70-74, with 75+ as the terminal open-ended age group, then calculations for the $CCR_{b,x+,t}$ require the summation of the three oldest age groups to get the population age 65+ at time $t-k$:

$${}_{\infty}CCR_{75,i,t} = {}_{\infty}P_{75,i,t} / {}_{\infty}P_{65,i,t-k} \quad [7a]$$

The formula for projecting the population 75+ of area i for the year $t+k$ is:

$${}_{\infty}P_{75+,i,t+k} = {}_{\infty}CCR_{75,i,t} \times {}_{\infty}P_{65,i,t} \quad [7b]$$

In our study we use aged 60 years and over as the terminal, open-ended age group. Numbers at older ages are sparse for the population of interest and mis-reporting and other errors are reduced by selecting 60 and over.

To show that the CCR method satisfies the fundamental demographic equation, we restate equation [2] using the

terms in equation [1]: $P_{i,t+k} = P_{i,t} + B_i - D_i + I_i - O_i$ where,

$P_{i,t}$ = Population of area i at time t (the launch year),

$P_{i,t+k}$ = Population of area i at time $t+k$ (the projection year),

B_i = Births in area i between time t and $t+k$,

D_i = Deaths in area i between time t and $t+k$,

I_i = In-migrants in area i between time t and $t+k$, and

O_i = Out-migrants in area i between time t and $t+k$,

then,

$${}_nCCR_{x,i,t} = ({}_nP_{x-k,i,t-k} + B_i - D_i + I_i - O_i) / {}_nP_{x-k,i,t-k} \quad [8]$$

Since we can also express equation [3] in terms of equation [1]:

$${}_nP_{x+k,i,t+k} = (({}_nP_{x-k,i,t-k} + B_i - D_i + I_i - O_i) / ({}_nP_{x-k,i,t-k})) \times ({}_nP_{x,i,t}) \quad [9]$$

where $x+k \geq 10$, then,

${}_nCCR_{x,i,t} = ({}_nP_{x-k,i,t-k} - D_i + I_i - O_i) / {}_nP_{x-k,i,t-k}$, and since

$N_i = I_i - O_i$, where $x+k \geq 10$, we have

$${}_nCCR_{x,i,t} = ({}_nP_{x-k,i,t-k} - D_i + N_i) / {}_nP_{x-k,i,t-k} \quad [10]$$

Equations [8], [9], and [10] show that the CCR Method is not only consistent with the fundamental demographic equation, but also closely related to the cohort-component method.

The CCR Method simply expresses the individual components of change—births, deaths, and migration—in terms of CCRs. As such, it satisfies the fundamental demographic equation. As we will see in the following section, this way of expressing the components of population change can be exploited. An important reason for a demographic forecasting method to be consistent with the fundamental demographic equation is to minimize the

potential errors associated with hidden heterogeneity (Vaupel and Yaushin 1985).

Because the US Census data are reported primarily in 10-year age groups for 1850 and 1860 (as can be seen in Table 1) we developed CCRs for these age groups rather than 5-year age groups. Table 2 provides the same data found in table 1 along with the 1850-1860 CCRs and the 1870 forecast.

RESULTS AND DISCUSSION

TABLE 2. MISSISSIPPI WHITE MALES IN 1850 & 1860 WITH 1850-60 CCRs & A FORECAST OF EXPECTED NUMBERS BY AGE TO 1870				
AGE	1850	1860	CCR	FORECAST (EXPECTED) 1870
0-9	50,913	55,945	0.72279	63,976
10-19	36,952	44,490	0.87384	48,887
20-29	27,164	32,911	0.89064	39,625
30-39	19,001	21,380	0.78707	25,903
40-49	11,378	14,375	0.75654	16,175
50-59	6,607	8,820	0.77518	11,143
60+	4,045	5,622	0.52779	7,622
TOTAL	156,060	183,543		213,331

See text for explanations of the methods.

Table 3 provides the difference between the projected 1870 population of white males by age and the 1870 census counts by age.

As can be seen in Table 3, there are 26,487 fewer white males found in 1870 than expected (-12.42%). Not surprisingly, the largest deficits are found in the age groups most likely to have served in the Confederate army, with almost 17 percent fewer (6,664) in age group 20-29, almost

28 percent fewer (7,226) in age group 30-39 and over 19 percent fewer (3,115) in age group 40-49. Also, there are 1,978 fewer (-17.75%) in age group 50-59. The reduction in the males of reproductive age likely accounts for the deficit of white males aged 0-9 (1,981 fewer than expected, a relative deficit of 3.5 percent).

TABLE 3. DIFFERENCE BETWEEN ACTUAL & EXPECTED NUMBERS OF MISSISSIPPI WHITE MALES FOR 1870 BY AGE				
AGE	1870 CENSUS (ACTUAL)	1870 FORECAST (EXPECTED)	DIFFERENCE: ACTUAL - EXPECTED	PERCENT DIFFERENCE
0-9	54,754	63,976	-9,222	-14.41%
10-19	50,409	48,887	1,522	3.11%
20-29	32,961	39,625	-6,664	-16.82%
30-39	18,677	25,903	-7,226	-27.90%
40-49	13,060	16,175	-3,115	-19.26%
50-59	9,165	11,143	-1,978	-17.75%
60+	7,818	7,622	196	2.57%
TOTAL	186,844	213,331	-26,487	-12.42%

Of interest is the fact that there are no deficits in age groups 10-19 and 60 years and over. Those in the age groups were highly unlikely to have served in the Confederate army. This suggests that in the absence of the war, the numbers of men in the age groups that were likely to have served would have been much larger. The relatively small differences between the actual and expected numbers for these two age groups also serves to support the fundamental argument of this paper, namely that the civil war's demographic impact on white males in Mississippi who were "of age" to serve in the war was substantial.

Although judged by many to be incomplete (e.g., Hacker 2014), the number of men from Mississippi who were killed in battle, died of wounds, and died of disease is estimated to be 15,265 (Fox 1889).³ Given that all of them were white males, we can compare this total to the sum of the differences between actual and expected for those in 1870 who were aged 20-59, which is higher at 18,983, as is the sum of the differences for those aged 20-49 in 1870, 17,005. Given that very little of either of these two differences is due to net out-migration, the comparisons suggest that deaths from all causes to white males from Mississippi who served in the Confederate army is on the order of 11 to 24 percent higher than the estimate of 15,265.

Table 4 compares the actual 1860-1870 CCRs with those used in the forecast (the 1850-60 CCRs). In no age group does a CCR exceed 1.00. This suggests two things. First, there was no net in-migration of white males in either

the 1850-60 period or the 1860-70 period; and, second, that mortality was high among those likely to have served in the Confederate army. For example, the 1850-60 CCR for those aged 30-39 is .78707, which is well above the 1860-70 CCR of .56750 for this same age group. One expects to see CCRs far less than 1.00 for the older age groups (e.g., 60 and over), but the presence of CCRs far less than 1.00 for those aged 20-29 to 50-59 in 1870 indicate that they were affected by a significant event – the Civil War.

TABLE 4. ACTUAL 1860-70 CCRs & THE 1850-60 CCRs USED TO PROJECT THE 1860 POPULATION TO 1870		
AGE	ACTUAL CCR 1860-70	1850-60 CCR APPLIED TO 1860 POPULATION
0-9	0.65676	0.72279
10-19	0.90105	0.87384
20-29	0.74086	0.89064
30-39	0.56750	0.78707
40-49	0.61085	0.75654
50-59	0.63757	0.77518
60+	0.54134	0.52779

DISCUSSION

Hacker (2011: 348) observes that “The human cost of the Civil War was greater than historians have long believed.” Our results suggest that the war had a substantial demographic impact on white males in Mississippi who were of military age during the war. The combined effects of depressed fertility, high mortality, and, possibly, net out-migration, yielded numbers far short of the expected numbers for men aged 20 to 59 in 1870. The overall impact is that 26,487 fewer white males were found in 1870 relative to what would have been expected had the 1850-60 trends (as exemplified by the 1850-60 CCRs) not been so severely affected by the Civil War. While our analysis suggests that the war had a substantial demographic impact on the white male population of Mississippi, it remains an open question how it affected the state’s white females as well as its African-American population.

In a response to Marshall (2014) who argues that Civil War deaths are greatly exaggerated, Hacker (2014) points out that it was the greatest demographic shock in U.S. history and that it deserves more study because we still lack a good understanding of it.

Our results lead us to suggest that the broader approach suggested by Hacker (2014) should be taken in order to estimate the demographic impact of the Civil War, one that goes beyond direct and indirect mortality. The work of Holmes and Vinoskis (1992), as well as that of Neely (2007), provides a starting point. We need, however, to extend it. Hacker (2014) suggests that we can do this by studying the effects of the war and its immediate aftermath on: (1) civilian deaths, especially among the African American population transitioning from slavery; (2) marriage and widowhood; (3) orphanhood; (4) family structure; (5) migration; and (6) the onset of the fertility transition.

We could further specify these suggestions by noting that: (1) war-based mortality levels among soldiers may have reduced fertility through a “marriage squeeze” (in this case a “squeeze” due to fewer males than females in the reproductive age groups) and related social mechanisms; (2) the war may have reduced immigration to the US as a whole as well as both immigration and domestic in-migration to the states particularly impacted by it; and (3) the war may have increased out-migration rates from states particularly impacted by it. While it may be difficult to isolate the war’s impact on fertility, mortality, and

migration separately, we believe that the approach illustrated here can provide reasonable estimates of its impact on these components of population change taken as a whole. As such, our approach provides a means of gaining a new perspective on the war’s demographic impact.

ENDNOTES

An online version of Fox’s work can be found at a site maintained by Tufts University (Gregory Crane is the editor in chief of a series of historical documents, under which this report is found): <http://www.perseus.tufts.edu/hopper/text?doc=Perseus%3Atext%3A2001.05.0068%3Achapter%3D16>. The estimate of Confederate casualties from all causes by state is taken from a compilation assembled by US General, James B. Fry, which can be found at <https://books.google.com/books?id=UQdPUMWfdM4C&pg=PA301&dq=%22james+b+fry%22+Confederate+state+s+of+america%22&hl=en&sa=X&ved=0ahUKEwj867XC8ozKAhVB5GMKHdy6As0Q6AEIHTAA#v=onepage&q=%22james%20b%20fry%22%20Confederate%20states%20of%20america%22&f=false>

The authors are grateful to the reviewers for comments that improved this paper.

LITERATURE CITED

- Faust, D. (2006). Numbers on top of numbers: Counting the Civil War dead. *Journal of Military History* 7, 997.
- Fox, W. F. (1889). *Regimental Losses in the American Civil War, 1861-1865: A Treatise on the extent and nature of the mortuary losses in the Union regiments, with full and exhaustive statistics compiled from the official records on file in the state military bureaus and at Washington*. Albany, NY: Albany Publishing Company.
- George, M., S. Smith, J. Tayman, and D. Swanson. (2004). Population Projections.” pp. 561-601 in J. Siegel and D. Swanson (eds.) *The Methods and Materials of Demography, Condensed Edition, Revised*. Academic/Elsevier Press: Los Angeles.
- Hacker, J.D. (2011). A Census-based count of the Civil War dead. *Civil War History* 57, 307-348.
- Hacker, J.D. (2014). Has the demographic impact of Civil War deaths been exaggerated? *Civil War History* 60, 453-458.

- Hamilton, C. H. and J. Perry (1962). A short method for projecting population by age from one decennial census to another. *Social Forces* 41, 163-170.
- Holmes, A. and M. Vinoskis (1992). The impact of the Civil War on southern marriage patterns. pp. 62-85 in S. South and S. Tolnay (eds.) *The changing American family*. Boulder, CO: Westview Press.
- Land, K. (1986). Methods for national population forecasts: A review. *Journal of the American Statistical Association* 81, 888-901.
- Marshall, N. (2014). The great exaggeration: death and the Civil War. *Journal of the Civil War Era* 4, 3-27.
- Neely, M. (2007). *The Civil War and the limits of destruction*. Cambridge, MA: Harvard University Press.
- Smith, S., J. Tayman, and D. Swanson. (2013). *A practitioner's guide to state and local population projections*. Springer B.V. Press. Dordrecht, Heidelberg, London, and New York.
- Swanson, D. (2008). "The demographic effects of hurricane Katrina on the Mississippi gulf coast: an analysis by zipcode." *Journal of the Mississippi Academy of Sciences*. 53, 213-231.
- Swanson, D. and J. Tayman (2012). *Subnational population estimates*. Springer B.V. Press. Dordrecht, Heidelberg, London, and New York.
- Swanson, D. and L. Tedrow (2012). Using cohort change ratios to estimate life expectancy in populations with negligible migration: A new approach. *Canadian Studies in Population* 39, 83-90.
- Swanson, D. A. Schlottmann, and R. Schmidt. (2010). Forecasting the population of census tracts by age and sex: An example of the Hamilton-Perry method in action. *Population Research and Policy Review* 29, 47-63.
- Swanson, D., L. Tedrow, and J. Baker (forthcoming). Exploring Stable Population Concepts from the Perspective of Cohort Change Ratios: Estimating the Time to Stability and Intrinsic r from Initial Information and Components of Change. In R. Schoen (ed.). *Dynamic Demographic Analysis*. Springer B.V. Press. Dordrecht, Heidelberg, London, and New York.
- Swanson, D., R. Forgette, J. McKibben, M. Van Boening, and L. Wombold (2009). The socio-demographic and environmental effects of Katrina: an impact analysis perspective. *The Open Demography Journal*, 2, 36-46.
- U.S. Census Bureau (no date) Census of Population and Housing (by Year, 1790 to 2010 (<http://www.census.gov/prod/www/decennial.html?cssp=SERP>)
- Vaupel, J. and A. Yaushin. (1985). Heterogeneity's ruses: Some surprising effects of selection on population dynamics. *The American Statistician* 39, 176-185.
- Vinovskis, M. (1989). Have social historians lost the Civil War? Some preliminary demographic speculations. *Journal of American History* 76, 34-59.

Evaluation of Drought Tolerant Maize Germplasm to Induced Drought Stress

Chathurika Wijewardana, W. Brien Henry, and K. Raja Reddy

Department of Plant and Soil Sciences, Mississippi State University, Mississippi State, MS 39762, USA

Corresponding Author: K. Raja Reddy, E-mail: krreddy@pss.msstate.edu

ABSTRACT

Corn is highly dependent upon soil moisture availability to generate consistent and favorable yield. The objective of this study was to assess photosynthesis responses of corn hybrids to drought stress intensities with and without known drought tolerance mechanisms. The six commercial hybrids, three drought tolerant, DKC 65-81, P1498, and N75HGTA, and three standards hybrids with similar maturities, P1319, DKC 66-97, and N77P3111, were grown in four sunlit, controlled environmental chambers for 38 days. Four variable soil moisture treatments were achieved by manipulating irrigation based on evapotranspiration of control treatments starting at two weeks after planting. Plant biomass was measured at the final harvest, 38 days after planting. Leaf gas exchange parameters were measured five times during the stress treatment period. Photosynthesis, stomatal conductance, and transpiration rates declined in all corn hybrids with declining soil moisture levels. Even though significantly higher values of these gas exchange parameters were observed under optimum and across a wide range of soil moisture conditions for the drought tolerant hybrids compared to non-drought hybrids, the rate of declines of these parameters with unit decrease in soil moisture content were not different between the two groups of hybrids. These results suggest that greater rates of gas exchange properties and associated biomass production was achieved by increasing the potential photosynthesis under optimum conditions. The stress response, however, is not modified among the two groups of corn hybrids. This suggests that breeding should focus not only increasing potential photosynthesis, but also its response to drought conditions to be able to produce higher biomass and greater yield.

Key words: Drought tolerance, maize, photosynthesis, droughtgard, aquamax, artesian

Abbreviations: DAP, Days after planting; SPAR - Soil-Plant-Atmosphere-Research; TD, Total dry weight; Pn, Photosynthesis; g_s , stomatal conductance; Tr, Transpiration rate; F_v'/F_m' , fluorescence; WUE, Water-use efficiency

INTRODUCTION

Corn (*Zea mays* L.) is among the top three of the most widely grown crops in global agriculture with a total production of 960 million metric tons in 2015 (USDA, 2016). The United States (U.S.) produces more than 40% of the world's corn, with the majority of the crop grown in the Heartland region including Illinois, Iowa, Indiana, South Dakota, and Nebraska. Corn production in the U.S. has risen over time because of new, improved varieties, pesticides, fertilizers, enhanced mechanization and production practices, and better management decisions. However, food demand for a growing global population is increasing pressure on prime arable land. Because of the increased demand for corn grain, rotational benefits, and declining cotton and soybean commodity prices, corn is often grown in sub-optimal regions that experience frequent drought. Research to screen and identify genotypes with improved drought tolerance has therefore, become important in the current and projected climatic conditions.

The Alluvial Aquifer serves as the major source of irrigation water for corn production in the U.S. Mid-south region; however, due to the recent expansion of irrigated acreage, it is declining at a rate of 300,000 acre feet per year (Rawson, 2015). Despite decreasing ground water levels, erratic precipitation patterns due to climate change has also become a significant challenge for corn production in the region. Water requirement for corn varies throughout its lifecycles but typically, a total 250 L of water is consumed by corn plant during the growing season (Du Plessis, 2003). The water requirements peak at the reproductive stage, with the most crucial water requirement occurring the two weeks before and after pollination (Nielson, 2013). Even though the corn reproductive stages are most sensitive to water deficiency, proper seedling establishment and early growth stages are also important to carry out all physiological and metabolic processes to develop canopy for maximum solar radiation interception and thus to avoid any yield losses.

Drought stress negatively affects corn productivity

causing a myriad of alterations on the morphological, biochemical and physiological processes of the plant (Sah et al., 2017; Reddy et al., 1997; Reddy et al., 2004). Thus, a prolonged water deficit during early canopy development reduces growth and yield considerably. Previous studies have evaluated a number of corn germplasm sources in response to drought stress (Bruce et al., 2002; Cakir, 2004; Efeoglu et al., 2009, and Lopus et al., 2011). Seed germination and early plant development (Wijewardana et al., 2015) are the first and foremost critical stages of crop establishment which affected both quality and quantity of crop yield. Many studies on the effects of drought stress on maize have demonstrated that water stress leads to significant reductions in plant height, leaf area, root growth, and grain yield (Anjum et al., 2011; Jama and Ottman, 1993; Kamara et al., 2003). Reduction in leaf growth and whole plant leaf area development lead to decreased light interception that impairs the photosynthetic efficiency and dry weight production (Brand et al., 2016; Nam et al., 1998; Stone et al., 2001). Distinctive differences in response to drought stress have also been recognized for a range of physiological characteristics, including reduced photosynthesis, stomatal activity, transpiration rate, and osmotic adjustment in the whole plant (Anjum et al., 2011). Insufficient soil moisture content reduces stomatal conductance which decreases the intake of CO₂ in to the leaf resulting in reduced photosynthesis (Cornic et al., 2000). Chlorophyll and carotenoid content and leaf electrolyte leakage have also been used as markers to assess drought stress tolerance in numerous plant species. Identifying the corn hybrids for enhanced drought tolerance requires an understanding of the morphological and physiological mechanisms and as well as genetic control of the relevant traits at different plant developmental stages (Bruce et al., 2002). Therefore, selection for improved traits under water limited conditions by using the fast, reproducible screening techniques appears to be the key to successfully evaluate germplasm for drought stress.

Over the years, seed companies and corn breeders have attempted to improve and introduce newer hybrids with greater stress tolerance and higher yield potential, and improved traits and breeding selections which can adapt to stressful growing conditions (Bruce, 2002). The newest technologies that the seed companies have developed are ‘Optimum[®] AQUAmax[™]’ marketed by Pioneer, ‘Genuity[®] DroughtGard[™]’ marketed by Monsanto, and ‘Agrisure[®] Artesian[™]’ marketed by Syngenta. The

AQUAmax hybrid which was developed by DuPont Pioneer have increased stomatal conductance to limit transpiration, higher photosynthetic production, vigorous ear silking, and prolific root system under water limited conditions. Also, from a three year study, Gaffney et al. (2015) found that under drought conditions, AQUAmax hybrids showed a 5 to 9% grain yield increase over non-drought tolerant conventional hybrids. The DroughtGard technology was developed by Monsanto and is the first transgenic drought tolerant hybrids. These hybrids express a cold shock protein derived from *Bacillus subtilis* to act as a chaperone that activates following plant exposure to drought stress (Castiglioni et al., 2008). A lower transpiration rate, higher plant water use efficiency, and increased grain yield have also been reported in DroughtGard hybrids against nondrought tolerant hybrids (Nemali et al., 2015). An increased grain yield has also been reported under moderate to severe drought stress conditions with Agrisure Artesian technology developed by Syngenta. From a field study conducted at 50% available water, Becker et al. (2011) found a continuous grain yield increase with Artesian technology as plant population density increased. Therefore, these technologies have shown yield stability by improving crop tolerance to drought.

A systematic evaluation of diverse corn germplasm is essential to identify and select for genotypes with improved tolerance and to elucidate the mechanisms underlying drought tolerance that can be used for maize breeding programs. Currently, there is an increasing trend to identify the crop plants tolerant to drought stress, which helps in meeting the food demands for increased global population. Hence, the objectives of this study were to compare the agronomic performance of commercially available corn hybrids designated with varying levels of drought tolerance and to evaluate their relative responses based on the photosynthetic dynamics under variable water limited conditions.

MATERIAL AND METHODS

Experimental Conditions and Plant Materials

This study was conducted in four sunlit Soil–Plant–Atmosphere–Research (SPAR) chambers located at the Rodney Foil Plant Science Research facility of Mississippi State University (33°28' N, 88°47' W), Mississippi State, MS, USA. Each SPAR chamber consists of a 1.27 cm thick Plexiglas chamber (2.5 m tall by 2 m long by 1.5 m wide) to house aerial plant parts and a steel soil bin (1 m deep by

2 m long by 0.5 m wide) to accommodate the root system. The Plexiglas allows 97% of the visible solar radiation to pass without spectral variability in absorption (Zhao et al., 2003). Throughout the experiment, the incoming daily solar radiation (285–2800 nm) outside of the SPAR units was measured with a pyranometer (Model 4-8; The Eppley Laboratory Inc., Newport, RI) and ranged from 3.5 to 28.40 MJ m⁻² d⁻¹ with an average of 15.95 ± 1.26 MJ m⁻² d⁻¹. These units have the capacity to precisely control air temperatures and chamber atmospheric CO₂ concentration at predetermined set points and at near ambient levels of photosynthetically active radiation (PAR). Air temperature in each SPAR chamber was set in to 30/22 °C (day/night) and monitored and adjusted every 10 s throughout the day and night and maintained within ± 0.5 °C of the treatment set points measured with aspirated thermocouples. The daytime temperature was initiated at sunrise and returned to the nighttime temperature 1 h after sunset. The relative humidity of each chamber was monitored with a humidity and temperature sensor (HMV 70Y, Vaisala, Inc., St. Louis, MO) installed in the returning path of airline ducts. From the air temperatures and relative humidity measurements, vapor pressure deficits were estimated as per the methods outlined by Murray (1967). Chilled mixture of ethylene glycol and water was injected through the cooling coils located outside the air handler of each chamber via several parallel solenoid valves that opened or closed depending on the cooling requirement to maintain a constant humidity. Variable density shade cloths (Hummert Seed Co., St. Louis, MO) placed around the edges of the plant canopy, and were adjusted regularly to match canopy height and to eliminate the need for border plants. Also, there is a heating and cooling system connected to air ducts that pass conditioned air through the plant canopy to cause leaf flutter. More details of operation and control of the SPAR facility have been described by Reddy et al. (2001). The mean values of day/night temperature, chamber CO₂ concentration, and vapor pressure deficit are provided in Table 1.

Six corn hybrids, P1498 and P1319, (Pioneer Hi-Bred International, Inc., Johnston, IA) DKC 65-81 and DKC 66-97, (DeKalb, Monsanto Company, St. Louis, MO) N75HGTA and N77P3111 (Agrisure, Syngenta Crop Protection Inc., Greensboro, NC) with known drought tolerance variability were used for this study. From each seed company, two hybrids were selected: one hybrid with drought tolerance (P1498 AquaMax, DKC6581 DroughtGard, and N75HGTA Artesian) and the other

hybrids without any designated drought tolerance. Because isolines with and without only the drought modifications or selections were not obtainable for this study, the two hybrids selected from each company were of the same relative maturities. Seeds for each hybrid were sown on 16 May 2014 in PVC (polyvinylchloride) pots (6" diameter by 12" high) with a 500 g of gravel at the bottom of each pot and filled with the soil medium consisting of 3:1 sand: top soil classified as sandy loam (87% sand, 2% clay, and 11% silt). Each pot had a small hole at the bottom for excess water drainage. All seeds were treated with their respective company's seed treatment. The experiment design included five replications per each hybrid thus, 30 pots per each unit arranged as a complete randomized design in 10 rows with three pots per each row. In total, one hundred and twenty pots were used for the four drought stress treatments. Initially, four seeds were sown in each pot and six days after emergence; the plants were thinned to one per pot. Plants were fertigated with full-strength Hoagland's nutrient solution (Hewitt, 1952) delivered through an automated and computer-controlled drip irrigation system to ensure favorable nutrient and water conditions for plant growth.

Treatments

The treatments included four levels of irrigation, 100, 75, 50, and 25% and those were maintained based on percent evapotranspiration (ET) values recorded on previous day. The ET measured on a ground area basis (L d⁻¹) throughout the treatment period as the rate at which condensate was removed by the cooling coils at 900-s intervals (Reddy et al., 2001) by measuring the mass of water in collecting devices connected to a calibrated pressure transducer. The amount of water provided to each treatment was adjusted by changing the duration of irrigation and based on ET values recorded on the previous day. Initially, all the plants were irrigated with the same water of volume as in 100% ET treatment, and 14 days after planting (DAP), ET-based irrigation treatments were imposed until the harvest at 38 DAP.

Measurements

Soil Moisture Content and Growth Measurements

Throughout the experimental period, soil moisture contents were monitored using soil moisture sensors (5TM Soil Moisture and Temperature Sensor, Decagon Devices, Inc., Pullman, WA) inserted at a depth of 15 cm in five random pots of each soil moisture treatment. Plants were harvested 38 DAP and leaves and stems were separated

from roots to take individual dry weights. The separated leaves, stems, and roots were placed in an oven and dried at 75 °C for 72 h to obtain total dry weights (TD).

Gas Exchange and Fluorescence Measurements

Leaf net photosynthesis rate (Pn), stomatal conductance (g_s), transpiration rate (Tr), and chlorophyll fluorescence (F_v'/F_m'^ˆ) were measured seven times from 20 to 32 DAP, from the youngest fully expanded leaves between 10:00 and 01:00 h, from three individual plants per treatment, using an LI-6400 portable photosynthesis meter (Li-COR Inc., Lincoln, NE) with an integrated fluorescence chamber head (Li-COR 6400-40 leaf Chamber Fluorometer, Li-Cor Inc.). The temperature in the leaf cuvette was set to the respective daytime air temperature of each treatment and [CO₂] was controlled by the CO₂ injection system to match the 400 μmol mol⁻¹ [CO₂]. While measuring photosynthesis, the photosynthetically active radiation provided by a 6400-02 LED light source was set to 1500 μmol m⁻² s⁻¹ and relative humidity inside the cuvette was maintained at approximately 50%. The fluorescence measurements were made using the built-in leaf chamber fluorometer which used two red LEDs (center wavelength lies on 630 nm and a detector radiation lies at 715 nm in the photosystem II (PS II) fluorescence band). A flash of light (> 7000 μmol m⁻² s⁻¹) achieved by using 27 red LEDs was used to measure the maximal fluorescence (F_m'^ˆ). Rapid dark adaptation to measure minimal fluorescence (F_o'^ˆ) was achieved by turning off the actinic light while using the far red LED (center wavelength at 740 nm). The far red radiation drives photosystem-I (PSI) momentarily to help drain PSII of electrons. The software in the instrument provided data on the Pn, g_s, Tr, leaf internal CO₂ concentration (C_i), and calculated quantum efficiency by (open) PSII reaction centers in light (F_v'/F_m'^ˆ). The photosynthetic water-use efficiency of the plants was calculated as Pn/g_s at C_a = 400 μmol mol⁻¹ (ambient CO₂ concentration).

Statistical Analysis

Each corn hybrid had five replicates for each drought stress treatment (100, 75, 50, and 25% ET). The analyses of variance (ANOVA) were performed to assess the hybrid

× treatment effect on total dry matter, Pn, g_s, Tr, WUE, and F_v'/F_m'^ˆ using PROC MIXED procedure of SAS (9.4, SAS Institute Inc., Cary, NC) at α = 0.05 level of significance. The differences between control and treated means were separated by least square means of Fisher's protected least significant difference method. Replication nested within the treatments was considered as random effect. The regression analyses were carried out using SigmaPlot version 13 (Systat Software Inc., San Jose, CA). The relationships among the soil moisture content and different gas exchange and water-use efficiency parameters were tested for linear and sigmoidal functions and the best fit regressions were selected. The Pn, g_s, Tr, WUE, and F_v'/F_m'^ˆ values at saturated soil moisture content were used as a denominator for each hybrid to develop the relative index for each trait; so that the derived values range between relative scales of 0-1 as described by Reddy et al. (2008). Then, those values were regressed against soil moisture content to estimate the relative response of the studied gas exchange traits. This analysis was necessary to measure the differences among the corn hybrid to test whether they have similar response under ample and limited soil moisture conditions.

RESULTS

Experimental Conditions and Manipulation of Soil Moisture Stress Treatments

In this study, the various soil moisture treatments, monitored by soil moisture sensors was significantly different among various ET-based treatments (Table 1) and this facilitated for an accurate control of the four drought stress treatments in the SPAR chambers (Fig. 1) throughout the experimental period. This method enabled us to address the study objectives by quantifying plant response as affected by different ET-based irrigation treatments. There was a clear separation and significant differences among the four water stress regimes with soil moisture values ranging from 0.224 (100% ET) to 0.111(20% ET) m³ m⁻³ water per soil volume. The other environmental variables such as day and night average temperatures, carbon dioxide concentrations, and vapor pressure deficits, however, not significantly different among the treatments (Table 1).

Table 1. Treatments based on the percentage of daily evapotranspiration (ET) imposed at 14 d after planting, average soil moisture, mean daytime chamber CO₂ concentration, mean daylight temperature, and mean daylight vapor pressure deficits (VPD) during the experimental period for each treatment. Values are means ± SE.

<u>Measured parameters</u> [†]				
<u>Treatment,</u> <u>% ET</u>	<u>†Mean soil moisture,</u> <u>m³ m⁻³ soil</u>	<u>Day/night</u> <u>temperature,</u> <u>°C</u>	<u>Chamber CO₂</u> <u>concentration,</u> <u>μmol mol⁻¹</u>	<u>Mean daily</u> <u>VPD, kPa</u>
100	0.22 a	26.45a	415a	1.18a
75	0.19 a	27.31a	412a	1.26a
50	0.16 b	27.84a	410a	1.44a
25	0.11 c	26.52a	416a	1.36a

[†] Soil moisture values are averaged for each treatment from 14 to 38 days after planting. Values within a column with different letter are significantly different at P<0.05.

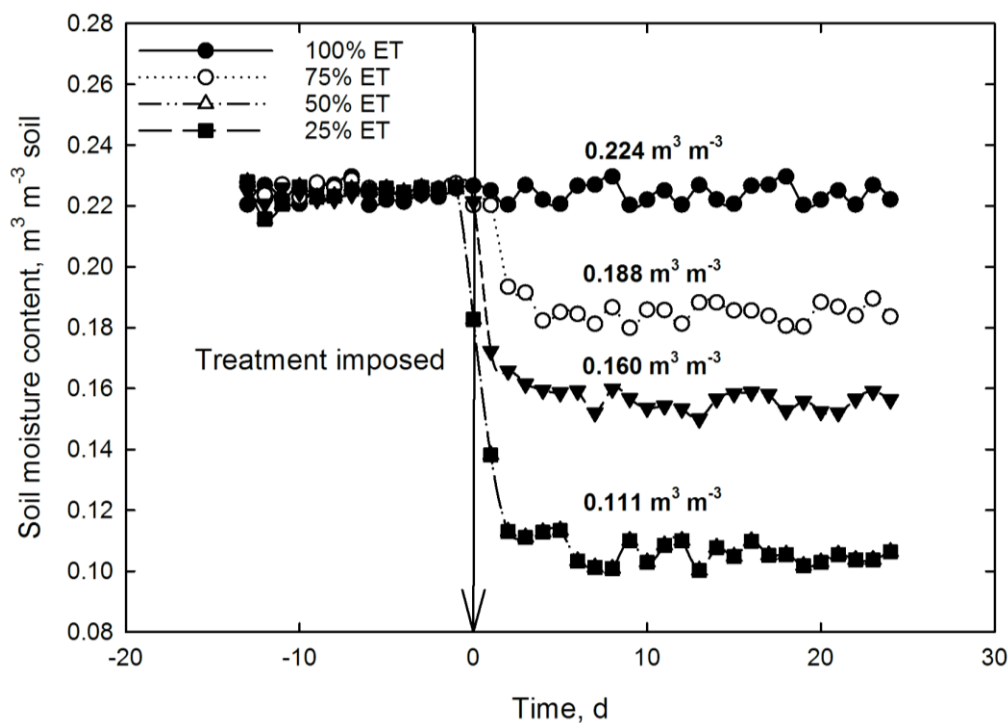


Figure 1: Volumetric soil moisture content across four drought stress treatments before and during the experimental period were maintained using sensor-based monitoring and irrigation system. The arrow indicates the day the treatments were imposed and the time when all the soil moisture levels reached the desired treatment levels. The average soil moisture values were given close to each treatment line for the period of drought (14-38 DAP).

Drought Stress and Gas Exchange Traits

Photosynthesis

In this study, net photosynthesis (P_n) decreased quadratically in all six corn hybrids with decreasing soil moisture content (Fig. 2). The three corn hybrids with drought genes or having drought tolerance traits, P1498, DKC 65-81, and N75HGTA, showed higher P_n values across all soil moisture levels compared to the other three corn hybrids without known drought traits (P1319, DKC 66-97, and N77P3111), across all soil moisture stress conditions. The hybrids, P1498, DKC 65-81, and N75HGTA exhibited about 43 to 46 $\mu\text{mol m}^{-2} \text{s}^{-1}$ under well-watered conditions compared to corn hybrids without those technologies. The photosynthesis response to soil moisture stress were, however, similar between the groups of corn hybrids (Fig. 2) declined by 46% at $0.05 \text{ m}^3 \text{ m}^{-3}$ soil compared to respective values at optimum soil moisture regimes of $0.2 \text{ m}^3 \text{ m}^{-3}$ soil.

Stomatal Conductance and Transpiration

Unlike photosynthesis response to soil moisture stress, stomatal conductance (g_s) and transpiration rates declined linearly in all corn hybrids with declining soil moisture content (Fig. 3). The g_s values were not significantly different among P1498, DKC 65-81, and N75HGTA corn hybrids, and similarly, g_s values among P1319, DKC 66-97, and N77P3111 were not significantly different among the two group (Fig. 3a). However, the intercepts values of the three corn hybrids, P1498, DKC 65-81, and N75HGTA, with drought traits were significantly different compared the intercept values for those corn hybrids (P1319, DKC 66-97, and N77P3111) without known drought tolerance mechanisms (Fig. 3a). The slopes of g_s , were not different between the groups with declining soil moisture levels. As expected, transpiration rate response between the two drought-tolerant groups showed similar responses to declining soil moisture levels (Fig. 3b); intercept being different and slopes being similar between the two groups of corn hybrids.

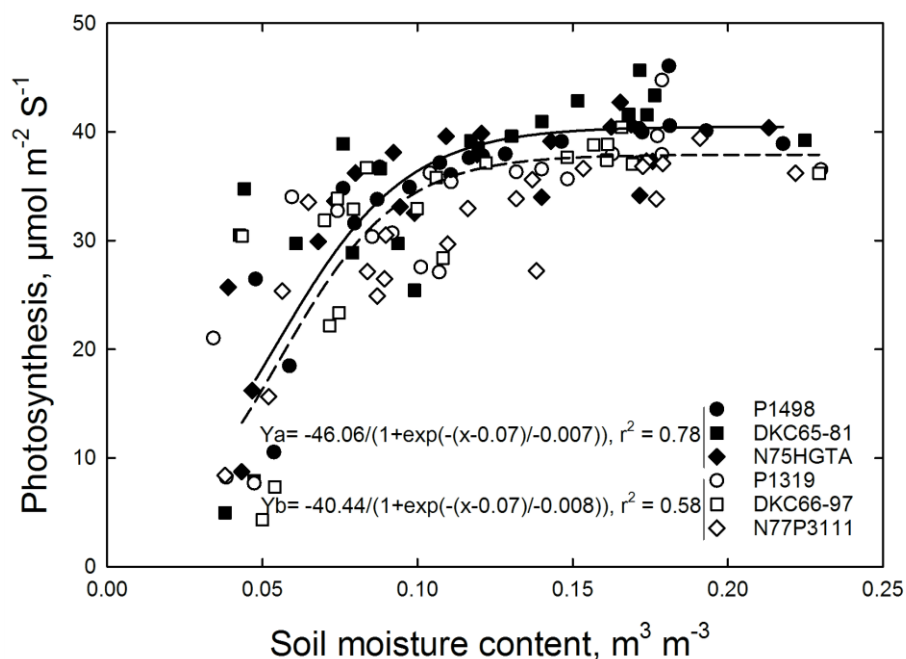


Figure 2. Soil moisture stress effects on plant net photosynthesis for the six corn hybrids. The solid line in the graph represents the quadratic regression for P1498, DKC6581, N75HGTA and given as Y_a , whereas dash line represents the quadratic regression for P1319, DKC6697, N77P3111 and given as Y_b correspondingly

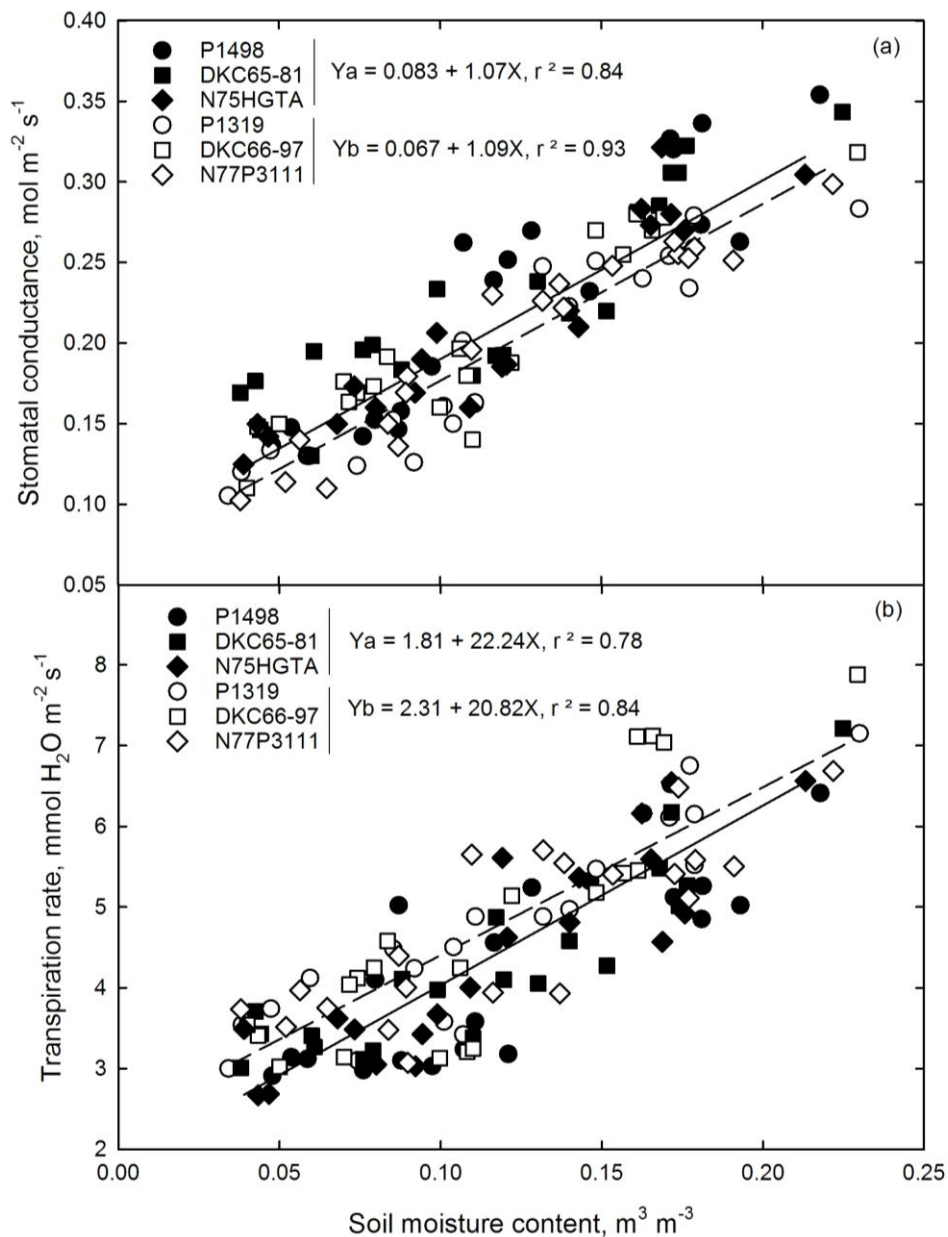


Figure 3. Soil moisture stress effects on (a) stomatal conductance and (b) transpiration rate for the six corn hybrids. The solid line in the graphs represents the linear regression for P1498, DKC6581, N75HGTA and given as Ya, whereas dash line represents the linear regression for P1319, DKC6697, N77P3111 and given as Yb correspondingly.

Water-Use and Quantum Efficiencies

In our study, unlike photosynthesis and stomatal conductance responses, water use efficiency (WUE) increased with declining soil moisture levels in all corn hybrids (Fig. 4a). The drought tolerant group of corn hybrids showed higher values across all soil moisture

levels compared to the non-drought counter parts corn hybrids. The slopes, however, were not different between the two groups and showed similar declines with increasing soil moisture levels.

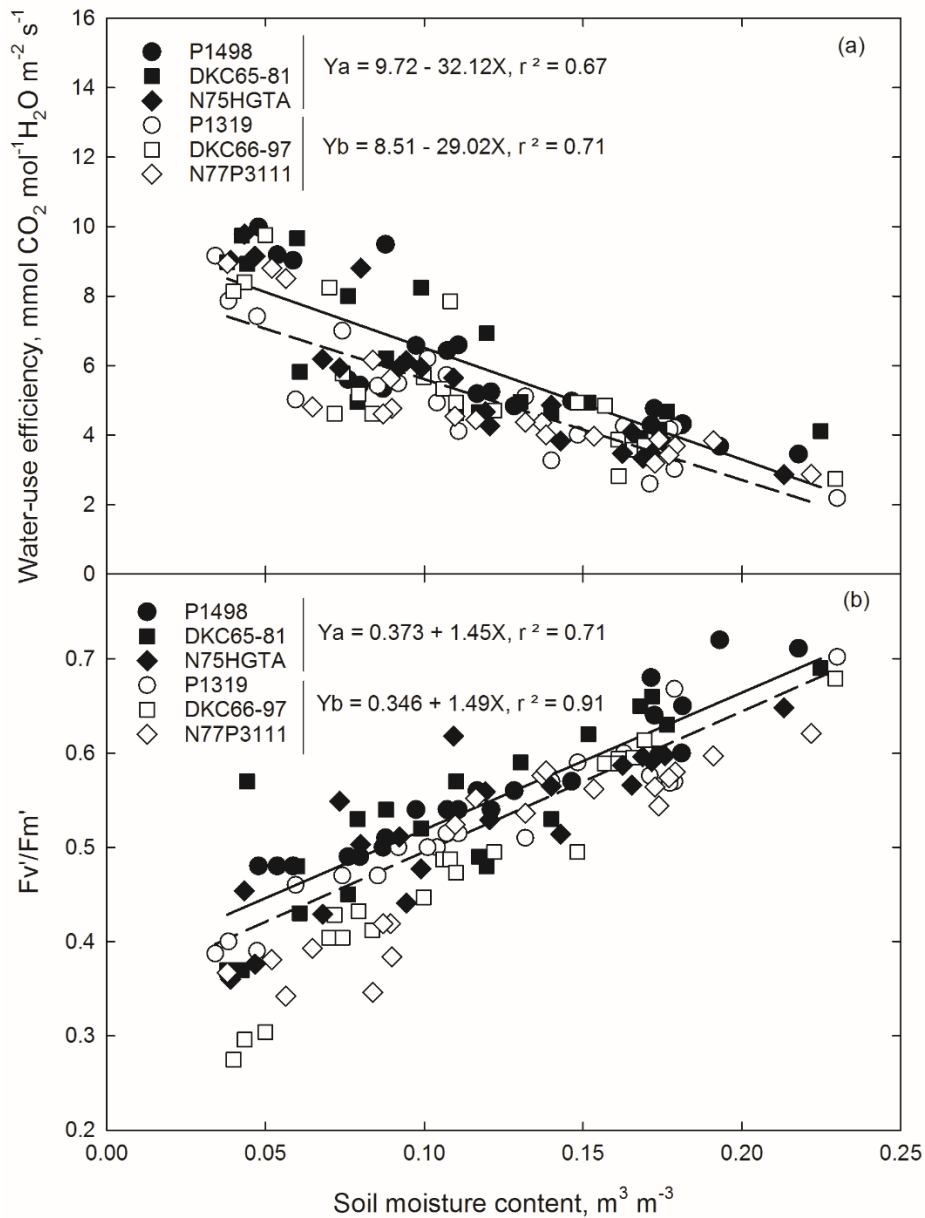


Figure 4. Soil moisture stress effects on (a) water-use efficiency and (b) fluorescence for the six corn hybrids. The solid line in the graphs represents the linear regression for P1498, DKC6581, N75HGTA and given as Y_a , whereas dash line represents the linear regression for P1319, DKC6697, N77P3111 and given as Y_b correspondingly.

Drought stress caused a linear decrease in leaf chlorophyll fluorescence (Fv/Fm') or the quantum efficiency among all the corn hybrids (Fig. 4b). Similar to all the gas exchange traits, the hybrids designated as drought tolerant (P1498, DKC 65-81, and N75HGTA) showed a significantly higher Fv/Fm' values across all soil moisture

levels compared to other three hybrids for leaf chlorophyll fluorescence. Even though, Fv/Fm' values at optimum soil moisture content were different among the two groups of corn hybrids, the slopes among the two groups were not different.

Relative Stress Indices

To understand the relative regulation of three drought tolerant and three non-drought tolerant hybrids under different soil moisture levels, the data on photosynthesis, g_s , Tr, WUE, and Fv'/Fm' were normalized using the procedure described by Reddy et al. (2008) (Fig. 5). Based on the results obtained, both the groups of corn hybrids showed that all the parameters declined similarly with one

function describing for each trait. The relative index for net photosynthesis exhibited an quadratic relationship with soil moisture content, while the relative indices for other parameters were declined linearly except water use efficiency which increased with declining soil moisture content. The corresponding regression parameters and coefficients are presented in Table 2 for all the gas exchange traits as a function of soil moisture content

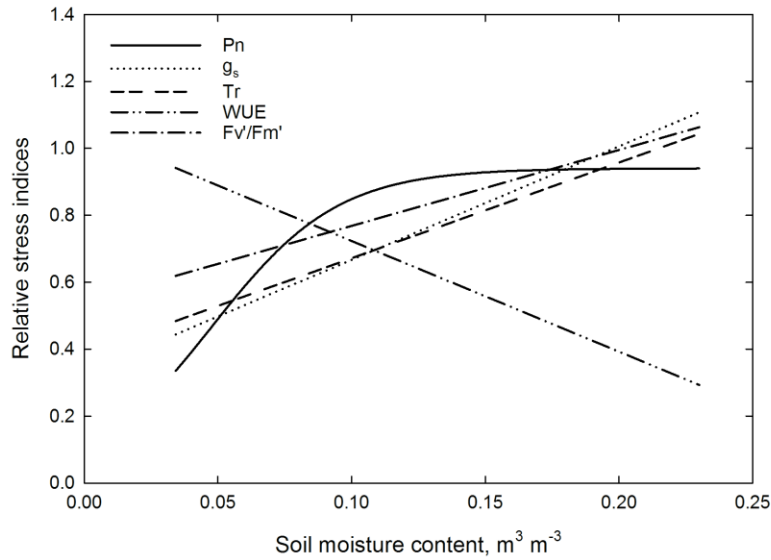


Figure 5. The relative stress response of each photosynthetic trait under different soil moisture stress levels. The relative index scale is ranged from 0 to 1 where the maximum values of photosynthesis, stomatal conductance, transpiration, water-use efficiency, and fluorescence at saturated soil moisture content was used as a denominator for each hybrid to develop the relative index for each of the trait.

Table 2. Regression (a, b, and c) parameters and regression coefficient (r^2) of gas exchange parameters for corn hybrids using all evapotranspiration (ET) based irrigation treatments to estimate relative stress indices as a function of soil moisture content.

<u>Gas exchange parameters</u>	<u>Regression parameters</u>			<u>Determination coefficient, r^2</u>
	a	b	c	
Photosynthesis (Pn)	0.94	0.02	0.05	0.70
Stomatal conductance (g_s)	0.33	3.39	--	0.80
Transpiration (Trans)	0.39	2.86	--	0.70
Water-use efficiency (WUE)	1.05	-3.31	--	0.72
Florescence (Fv'/Fm')	0.54	2.69	--	0.71

DISCUSSION

Studies on gas exchange and water use efficiency traits under different soil moisture stress levels are important tools to achieve a more refined selection of tolerant cultivars, which could lead to higher plant productivity under variable drought conditions. In this study, a strong and positive correlation observed between mean photosynthesis under each treatment and corn hybrid and total plant dry matter production (Fig. 6) indicated the importance of photosynthesis for dry matter production and thus to yield. Therefore, understanding photosynthesis and photochemical properties of the corn hybrids and their relative responses to drought conditions are important to further develop new hybrids for drought tolerance. Many studies have reported that drought tolerant corn hybrids attained more dry weights as compared to drought sensitive corn hybrids (Athar and Ashraf, 2005; Farooq et al., 2009; Sallah et al., 2002; Wijewardana et al., 2016a) with greater photosynthesis similar to our studies with varied drought tolerant corn hybrids and under different levels of soil moisture contents.

The drought induced reduction of photosynthesis has been extensively studied and reported for many plant species with the changes associated in plant physiology and metabolism (Foyer et al., 2009; Cornic et al., 2000; Ghannoum, 2009). The previous studies suggest that the decreased photosynthesis was associated with both stomatal and non-stomatal limitations (Wijewardana et al., 2016b). As the drought stress intensifies and continues, the uptake of CO₂ from the atmosphere is restricted due to stomatal closure, which, in turn, reduces the assimilation rate. Some recent studies reported an inactivation of the C₄ cycle enzymes located in the mesophyll chloroplasts due to higher oxidation during soil moisture stress which could lower the grain yield due to the photosynthesis inhibition

(Ghannoum, 2009). The reduction of photosynthesis under drought conditions in the present study are due to reductions in movement of CO₂ from the atmosphere to the site of carboxylation within the chloroplast (Lopes et al., 2011), or as photooxidation damages to the photosynthetic mechanism.

The maximum photosynthesis ($P_{n_{max}}$) is a key photosynthetic trait that characterizes the maximal photon utilization capacity of plants and consequently, reveals the net primary productivity. Based on our findings, the drought tolerant corn hybrids, P1498, DKC 65-81, and N75HGTA, exhibited maximum $P_{n_{max}}$ under both ample and in a wide range of soil moisture levels. After 0.15 m³ m⁻³ soil moisture level, both the drought tolerant and non-drought tolerant hybrids showed a larger reduction in photosynthesis, but the rate of decrease is comparatively similar among the two groups of corn hybrids. In other words, drought tolerant hybrids had greater potential photosynthesis; the rates of reduction (slopes) were similar between the two groups, drought tolerant and non-drought tolerant corn hybrids, indicating that the response to drought in the drought tolerant group of corn hybrids was not modified.

Stomatal closure is one of the first responses to water deficit to prevent transpirational water loss. From the results, it is clear that increased levels of soil moisture stress greatly lowered the stomatal conductance in all hybrids, and stomatal conductance declined linearly with declining soil moisture levels. Similar to photosynthesis response, the slopes of the stomatal decline between the two groups of corn hybrids were similar and the intercepts were different (Fig. 3a) indicating that the rates of stomatal response to drought were similar among the two groups. This shows that the response to drought has not been modified in the drought tolerant corn hybrids.

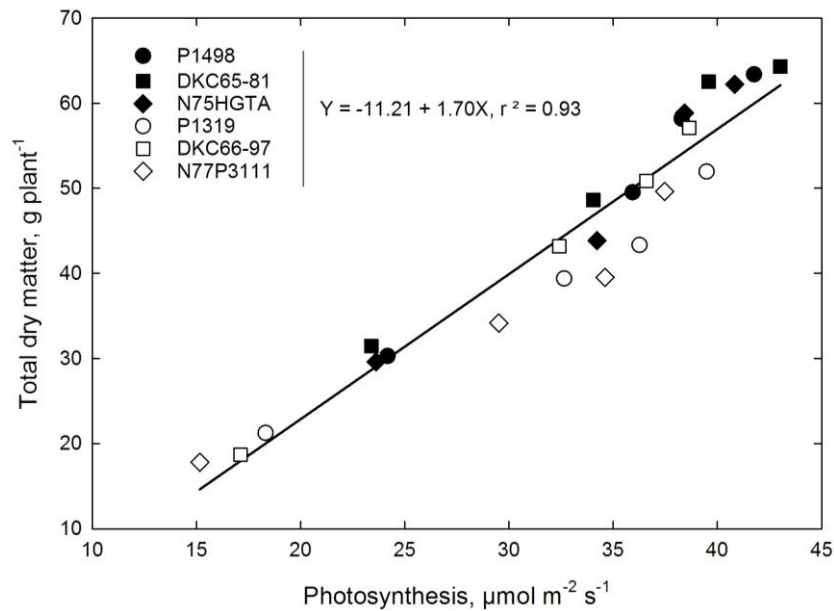


Figure 6. Correlation between photosynthesis, averaged over treatment for each corn hybrid, and plant dry matter production measured at the end of the experiment, 38 days after planting.

The maximum photosynthesis (Pn_{max}) is a key photosynthetic trait that characterizes the maximal photon utilization capacity of plants and consequently, reveals the net primary productivity. Based on our findings, the drought tolerant corn hybrids, P1498, DKC 65-81, and N75HGTA, exhibited maximum Pn_{max} under a wide range of soil moisture levels. After $0.15 \text{ m}^3 \text{ m}^{-3}$ soil moisture level, both the drought tolerant and non-drought tolerant hybrids showed a larger reduction in photosynthesis, but the rate of decrease is comparatively similar among the two groups of corn hybrids. In other words, drought tolerant hybrids had greater potential photosynthesis; the rates of reduction (slopes) were similar between the two groups, indicating that the response to drought in the drought tolerant group of corn hybrids was not modified.

Stomatal closure is one of the first responses to water deficit to prevent transpirational water loss. From the results, it is clear that increased levels of soil moisture stress greatly lowered the stomatal conductance in all hybrids, and stomatal conductance declined linearly with declining soil moisture levels. Similar to photosynthesis response, the slopes of the stomatal decline between the two groups of corn hybrids were similar and the intercepts were different (Fig. 3a) indicating that the rates of stomatal response to drought were similar among the two groups.

This shows that the response to drought has not been modified in the drought tolerant corn hybrids.

Decreased stomatal conductance under severe moisture level is identified as a drought response mechanism in order to minimize the water loss from the plant. There has been an extensive characterization of drought-induced decline of stomatal conductance in many plants. Still there are some ongoing debates if stomatal closure is a result of reduced soil moisture content or leaf water potential. The plant root system is the first sensitive organ to soil moisture deficit and is responsible for sending chemical signals like abscisic acid (ABA) to closing up the stomata, while the plant attempts to maintain a constant leaf water status (Taylor, 1991; Turner et al., 2001). As drought persists it limits continues to limit transpiration which may promote the accumulation of ABA resulting in an imbalance of leaf sap pH. Under drought stress, cytokinin has also been proposed to play a major role (Morgan, 1990) but behaving in an opposite way. The increase in ABA and decline in cytokinin concurrently weaken g_s which diminish the inflow of CO_2 into the leaves and releases more electrons for the formation of reactive oxygen species (ROS). These harmful ROS cause photo-oxidative damages to chloroplasts by braking cell membranes and chlorophyll leading to a photosynthesis (Foyer et al., 2009).

Previous studies have reported the decrease of transpiration rate under severe water deficit as a drought

avoidance mechanism which could be achieved through minimizing water loss by stomatal closure or decreasing the transpiring leaf surface by leaf rolling. Even though the drought tolerant hybrids had increased stomatal conductance under both optimum and severe stress conditions, the transpiration rate was lower compared to their non-tolerant hybrids. This was supported by increased water use efficiency among the tolerant hybrids. The increase of WUE may have resulted from lower transpiration rates under water deficit conditions. Increased WUE is a drought adaptive mechanism which enhances the tolerance of corn plants to water deficit. Supporting to our findings, drought tolerance was found to be associated with higher WUE which can maintain higher photosynthetic capacity under water deficiency conditions (Escalona et al., 1999). Hence, plants having higher WUE may be very suitable mainly for the plant production under water limited condition due to their reduced water use. This feature has been described as an important goal for crop breeding programs in order to induce drought tolerance and yield enhancement in water limited environments.

In the present study, increasing moisture stress levels caused a linear decrease in the F_v'/F_m' and affected significantly for the tolerant and non-tolerant hybrids. However, similar to other photosynthetic traits such as P_n , g_s , and WUE drought tolerant cultivars possessed higher F_v'/F_m' compared to their non-drought tolerant hybrids both under optimum and limited moisture levels. It is suggested that maintaining a higher F_v'/F_m' as a protective mechanism of the photosystem from photo-inhibitory damage which may lead to the repossession of photosynthesis after the plant is recovered from water stress. In the light reaction phase of photosynthesis, most of the excitation energy from the photosystem II (PSII) is converted into chemical energy through the linear electron transport. Upon de-excitation of the PSII, the excess energy is dissipated as heat and a small fraction is lost as fluorescence (Maxwell and Johnson, 2000). Therefore, increase in F_v'/F_m' in tolerant hybrids suggests that those hybrids kept more PSII centers in an open state so the more excitation energy will be utilized for electron transport. On the other hand, non-drought tolerant hybrids failed to maintain more PSII centers in open state, and therefore showed decreased F_v'/F_m' .

We evaluated six corn hybrids for their responses to four drought stress treatments. The plant responses to soil moisture stress under control and drought stress treatments were assessed using physiological parameters and total

biomass production. The hybrids designated as drought exhibited lower drought sensitivity with relatively higher photosynthesis, stomatal conductance, water use efficiency, and reduced transpiration rate compared to their non-tolerant hybrids both under optimum and stressed conditions. The higher rate of photosynthesis and WUE confers greater plant survival and more biomass accumulation under limited water condition. However, when the relative indices for measured traits were plotted against the soil moisture content, a similar response was shown by the both tolerant and non-tolerant hybrids towards the drought stress. This finding revealed that drought tolerance mechanisms are well functioned and expressed in the tolerant hybrids than their non-tolerant hybrids at the photosynthetic process levels and those could be useful to sustain the plant growth and the productivity under water limited condition. However, all the hybrids responded similarly in their photosynthetic behavior towards soil moisture deficit.

CONCLUSIONS

This study was conducted to evaluate the drought response of six corn hybrids with known drought tolerance in early vegetative growth. The hypothesis was that physiological plant processes will be influenced by different soil moisture levels and the corn hybrids considered drought tolerant will have more positive responses under soil moisture stress. Even though the drought tolerant corn hybrids, DKC 65-81, P1498, and N75HGTA, showed greater photosynthesis and other traits compared to non-drought corn hybrids, P1319, DKC 66-97, and N77P3111, the rates of decline in all these processes in response to drought were similar among the two groups of corn hybrids. This implies that the drought tolerant corn hybrids have greater potential photosynthesis under optimum conditions. It would have been beneficial if drought tolerant corn hybrid responses to drought were also different. Future breeding objectives should focus on developing corn hybrids with higher potential photosynthesis as well as with enhanced response to drought conditions.

ACKNOWLEDGEMENT

The authors would like to thank David Brand for technical assistance and Trip Walker of Syngenta, Chris Daves and Davie Wilson of Monsanto, and Jeff Hollowell and Dan Poston of Pioneer for providing seeds. Mention of trade names in this publication is exclusively for the purpose of providing specific information and does not imply

recommendation or endorsement by the U.S. Department of Agriculture. This research was partially funded by Mississippi Agricultural and Forestry Experiment Station, the Mississippi Corn Promotion Board, and the USDA-NIFA 2013-34263-20931, sub-award to Mississippi State University, G-7799-2. This article is a contribution from the Department of Plant and Soil Sciences, Mississippi State University, Mississippi Agricultural and Forestry Experiment Station.

LITERATURE CITED

- Anjum SA, Wang LC, Farooq M, Hussain M, Xue LL, Zou CM. Brassinolide application improves the drought tolerance in maize through modulation of enzymatic antioxidants and leaf gas exchange. *J. Agron. Crop Sci.* 2011; 197: 177-185.
- Athar HR, Ashraf M. Photosynthesis under drought stress. In: *Handbook of Photosynthesis*. (Ed.): M. Pessarakli, CRC Press, Taylor and Francis Group, New York. 2005; 793-804 pp.
- Becker J, Bean B, Xue Q, Marek T. 2011 Syngenta Artesian™ First Generation Drought Tolerant Corn Trial Progress Report". 06 Oct 2016. <http://amarillo.tamu.edu/files/2010/11/2011-Syngenta-Agrisure-trial.pdf>.
- Brand D, Wijewardana C, Gao W, Reddy KR. Interactive effects of carbon dioxide, low temperature, and ultraviolet-B radiation on cotton seedling root and shoot morphology and growth. *Front. Earth Sci.* 2016; 10: 607-620. Doi10.1007/s117-7-016-0605-0
- Bruce WB, Edmeades GO, Baker TC. Molecular and physiological approaches to maize improvement for drought tolerance. *J. Exp. Bot.* 2002; 53: 13-25.
- Cakir R. Effect of water stress at different development stages on vegetative and reproductive growth of corn. *Field Crop Res.* 2004; 89: 1-16.
- Castiglioni P, Warner D, Benson RJ, Anstrom DC, Harrison J, Stoecker M, Heard JE. Bacterial RNA Chaperones confer abiotic stress tolerance in plants and improved grain yield in maize under water-limited conditions. *Plant Physiol.* 2008; 147: 446-455.
- Cornic, G. Drought stress inhibits photosynthesis by decreasing stomatal aperture-not affecting ATP synthesis. *Trends Plant Sci.* 2000; 5: 187-188.
- Du Plessis, J. 2003. Maize production. Directorate of Agricultural Information Services, Department of Agriculture South Africa, 90 pp.
- Efeoglu B, Ekmekci Y, Cicek N. Physiological responses of three maize cultivars to drought stress and recovery. *South Afr. J. Bot.* 2009; 75: 34-42.
- Escalona, J.M., J. Flexas, and H. Medrano. Stomatal and non-stomatal limitations of photosynthesis under water stress in field-grown grapevines. *Aus. J. Plant Physiol.* 1999; 26: 421-433.
- Farooq M, Wahid A, Kobayashi N, Fujita D, Basra SMA. Plant drought stress: effects, mechanisms, and management. *Agron. Sustain. Dev.* 2009; 29: 185-212.
- Foyer CH, Bloom A, Queval G, Noctor G. Photo respiratory metabolism: genes, mutants, energetics, and redox signaling. *Ann. Rev. Plant Biol.* 2009; 60: 455-484.
- Gaffney J, Schussler J, Löffler C, Cai W, Paszkiewicz S, Messina C, Groeteke J, Keaschall J, Cooper M. Industry-scale evaluation of maize hybrids selected for increased yield in drought-stress conditions of the US corn belt. *Crop Sci.* 2015; 55: 1608-1618.
- Ghannoum, O. C4 photosynthesis and water stress. *Ann. Bot.* 2009; 103: 635-644.
- Hewitt EJ. 1952. Sand and water culture methods used in the study of plant nutrition. *Tech. Commun.* 22. Commonwealth Agric. Bur., Farnham Royal, UK.
- Jama AO, Ottman MJ. Timing of the first irrigation in corn and water stress conditioning. *Agron. J.* 1993; 85: 1159-1164.
- Kamara AY, Menkir A, Badu-apraku B, Ibikunle O. The influence of drought stress on growth, yield and yield components of selected maize genotypes. *J. Agric. Sci.* 2003; 141: 43-50.
- Lopes MS, Araus JL, Van Heerden PDR, Foyer CH. Enhancing drought tolerance in C4 crops. *J. Exp. Bot.* 2011; 62: 3135-3153.
- Maxwell K, Johnson GN. Chlorophyll fluorescence -a practical guide. *J. Exp. Bot.* 2000; 51: 659-668.
- Morgan PW. 1990. Effects of abiotic stresses on plant hormone systems, in: *Stress Responses in plants: adaptation and acclimation mechanisms*, Wiley-Liss, Inc. 113-146 pp.

- Murray FW. On the computation of saturation vapor pressure. *J. Appl. Meteorol.* 1967; 6: 203-204.
- Nam NH, Subbaroa GV, Chauhan YS, Johansen C. Importance of canopy attributes in determining dry matter accumulation of pigeon pea under contrasting moisture regimes. *Crop Sci.* 1998; 38: 955-961.
- Nemali, KS, Bonin C, Dohleman FG, Stephens M, Reeves WR, Nelson DE, Castiglioni P, Whitsel JE, Sammons B, Lawson M. Physiological responses related to increased grain yield under drought in the first biotechnology-derived drought-tolerant maize. *Plant Cell Environ.* 2015; 38: 1866-1880.
- Nielsen, RL. 2013. "Effects of Stress during Grain Filling in Corn". Corny News Network, Purdue University, West Lafayette. 08 Nov 2016. <http://www.agry.purdue.edu/ext/corn/news/timeless/grainfillstress.html>
- Rawson JC. Enhancing irrigation scheduling in the Mississippi delta through soil moisture monitoring and improved modeling capabilities. Master thesis. 2015; Mississippi State University.
- Reddy AR, Chaitanyaa KV, Vivekanandan M. Drought-induced responses of photosynthesis and antioxidant metabolism in higher plants. *J. Plant Physiol.* 2004; 161: 1189-1202.
- Reddy KR, Hodges HF, McKinion JM. Crop modeling and applications: a cotton example. *Adv Agron.* 1997; 59: 225-290.
- Reddy KR, Hodges HF, Read JJ, McKinion JM, Baker JT, Tarpley L, Reddy VR. Soil-plant-atmosphere-research (SPAR) facility: a tool for plant research and modeling. *Biotronics* 2001; 30: 27-50.
- Reddy, K.R., Hodges, H.F., McKinion, J.M. Crop modeling and applications: a cotton example. *Adv Agron.* 1997; 59: 225-290.
- Reddy, K.R., V.G. Kakani VG, H.F. Hodges HF. Exploring the use of environmental productivity index concept for crop production and modeling. In: L.R. Ahuja LR, V. Reddy V, S.A. Saseendran SA, and Q. Yu Q., editors, *Response of crops to limited water: Understanding and modeling of water stress effects on plant growth processes.* ASA, CSSA, and SSSA, Madison, WI. 2008; p. 387- 410.
- Sah, SK, Reddy KR, Li J. Abscisic acid and abiotic stress tolerance in crop plants. *Front. Plant Sci.* 2017; 7: 571.
- Sallah PYK, Antwi KO, Ewool MB. Potential of elite maize composites for drought tolerance in stress and non-drought stress environments. *African Crop Sci. J.* 2002; 10: 1-9.
- Stone C, Chisholm L, Coops N. Spectral reflectance characteristics of eucalypt foliage damage by insects. *Aust. J. Bot.* 2001; 49: 687-698.
- Taylor IB. Genetics of ABA synthesis In: Davies W.J., H.G., Jones (Eds.), *Abscisic acid: Physiology and Biochemistry*, Bios Scientific Publishers Ltd. UK. 1991; 23-38 pp.
- Turner NC, Wright GC, Siddique KHM. Adaptation of grain legumes (pulses) to water-limited environments, *Adv. Agron.* 2001; 71: 123-231.
- USDA. 2016. World agricultural production. Office of global analysis, foreign agricultural service, WAP 8-16. 12 Nov 2016
<http://apps.fas.usda.gov/psdonline/circulars/production.pdf>
- Wijewardana C, Henry WB, Gao W, Reddy KR. Interactive effects on CO₂, drought, and ultraviolet-B radiation on maize growth and development. *Photochem. Photobiol.* 2016a; 160: 198-209.
<http://dx.doi.org/10.1016/j.jphotobiol.2016.04.0>
- Wijewardana C, Henry WB, Hock M, Reddy KR. Growth and physiological trait variation among corn (*Zea mays* L.) hybrids for cold tolerance. *Can. J. Plant Sci.* 2016b; 96: 639-656.
<http://dx.doi.org/10.1129/CJPS-2015-0>
- Wijewardana C, Hock M, Henry WB, Reddy KR. Screening corn hybrids for cold tolerance using morphological traits for early season seeding. *Crop Sci.* 2015; 19: 75-78.
[doi:10.2135/Cropsci2014.07.0487](http://dx.doi.org/10.2135/Cropsci2014.07.0487)
- Wu Y, Cosgrove DJ. Adaptation of roots to low water potentials by changes in cell wall extensibility and cell wall proteins. *J. Exp. Bot.* 2000; 51: 1543-1553.
- Zhao D, Reddy KR, Kakani VG, Read JJ, Sullivan JH. Growth and physiological responses of cotton (*Gossypium hirsutum* L.) to elevated carbon dioxide and ultraviolet-B radiation under controlled environmental conditions. *Plant Cell Environ.* 2003; 26: 771-782.

Load Transfer Mechanisms Of Biostructures: A Complex Network Approach

Reena R. Patel¹, Guillermo A. Riveros¹, David S. Thompson²

¹-U.S. Army Engineer Research and Development, 3909 Halls Ferry Road, Vicksburg, MS 39180-6199

²-Mississippi State University, Mississippi State, MS 39762

Corresponding Author: Guillermo A. Riveros

ABSTRACT

Biostructures are unique compared to man-made structures owing to the multiple functions they are designed to accomplish coupled with the complex hierarchical geometrical arrangement that makes them strong, tough, lightweight, and energy dissipative. This work presents an integrated, interdisciplinary approach that utilizes computational and experimental mechanics with a complex network strategy to obtain fundamental insights into failure mechanisms of high performance, light weight, structured composites by investigating the effects of geometrical and material properties of the paddlefish rostrum. Although computational mechanics experiments give an overall distribution of stresses in the structural systems, due to the large numbers of degrees of freedom the underlying kinematics, which play a vital role in load transfer mechanisms and the formation of the strong and weak links in the network, are unknown and expensive to compute using traditional methods. To address this problem, the load transfer in the rostrum is formulated as a network flow problem. The nodes and edges of the network are extracted from the numerical model to generate the flow network. The flow network is weighted based on the parameter of interest, which are stresses in the current study. The changing kinematics of the system is input to the mathematical algorithm that will compute the maximum flow of the stresses at uniform cost. This research investigates the load transfer mechanisms for the rostrum of the paddlefish by conducting computational mechanics experiments; identify the formation of the force chains in the rostrum by employing maximum flow/minimum cut mathematical algorithm and demonstrate preliminary results of the advantages of the flow network to solve this type of engineering problems.

Keywords: Complex network, computational mechanics, rostrum, paddlefish, biostructure, hierarchical geometry

INTRODUCTION

Complex networks have been utilized to understand the dynamics of numerous complex systems such as traffic flow, energy flow through food webs in an ecosystem, communication networks, electrical networks, fluid flow through pipelines, community structure of company ownership, air transportation, patrol routing problems, failure of quasi-brittle materials, and force transmission in dense granular media [1, 2]; however, this method has not been employed to analyze the hierarchical geometry of living specimens. This work is the initial point in understanding the design and engineering of high performance, lightweight, structured composites by investigating the geometry and material properties of the paddlefish rostrum (Figure 1). Size, shape, and position of the rostrum helps generate the lift required by paddlefish for filter feeding and balance as demonstrated by Riveros et. al [3, 4, 5]. Recent numerical experiments have shown that the rostrum has superior energy dissipation and impact resistance characteristics when compared to a homogeneous material with identical geometry [6]. The superior performance of the rostrum is directly dependent on its complex hierarchical lattice architecture. The lattice is

formulated as an indeterminate, non-linear structure comprised of varying material types, and properties, with non-uniform stiffness and irregular shapes. Knowledge is lacking in how nature has geometrically optimized this lattice structure, which exhibits superior mechanical strength/resilience, and hydrodynamic efficiency. A transdisciplinary approach that utilizes the attributes from computational mechanics experiments and complex network algorithms will aid in developing a fundamental understanding of the role the redundant lattice architecture plays in achieving structural resiliency.

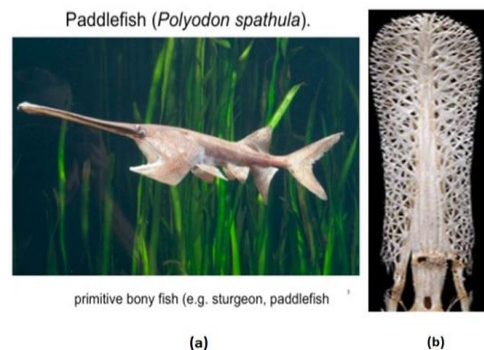


Figure 1: (a) Paddlefish (b) Paddlefish rostrum cartilage skeleton

METHODS AND DATA

The rostrum of the paddlefish, a species of ancient cartilaginous fish, displays unique strength, yet knowledge is lacking on what cellular and biochemical features interact during the fish's development to give the rostrum its unique strength. The uniqueness of the biological structures acquired due to the complex hierarchical lattice architecture coupled with heterogeneous constituents causes an uncertainty as to what is dictating the structural response. To uncover the underlying kinematics, this study will use the surface topology acquired from micro CT imagery and a weighing function based on strain and flow measurement, which are believed to be the most dependable data that can be measured since the force chains are short circuited. The rostrum is formulated as a network flow problem [7, 8]. To achieve this, a flow network graph $\mathbf{G} = (\mathbf{V}, \mathbf{E})$ is developed from the finite element model of the rostrum such that,

- \mathbf{V} represents the nodes obtained from the finite element model of the rostrum.
- \mathbf{E} represents the edges, connecting the nodes in \mathbf{V} , indicating the connectivity between the nodes.
- Each edge $(u, v) \in \mathbf{E}$ has a capacity \mathbf{C} associated with it, which is representative of the maximum amount of flow that could be transmitted through the edge.

We identify two nodes in the network to serve as the source, s , and target, t , nodes so the flow can be transmitted from the source node s to the target node t . The selection of these nodes will be dependent on the boundary conditions that will be applied to the rostrum. For example, if the rostrum is subjected to compression loading from the top and bottom, the source and target nodes can be selected from the top and bottom loading surfaces, respectively. From Newton's third law of motion it can be inferred that the transmission of flow along each edge is symmetric. Hence, the flow from source to target is identical irrespective of the choice of the source and target nodes. The methodology utilized in the current study and also the composition, material properties of the rostrum are described in detail in a

technical report by Patel et. al [9]. The technical report [9] also describes the modus operandi of the minimum cut maximum flow algorithm on a demonstration model created from the computational mechanics experiment on the rostrum.

RESULTS AND DISCUSSION

Based on the previously constructed model in [10], computational experiments are carried out with uniform pressure loading on rostrum using general static analysis in Abaqus/Standard [11]. Experimental details are provided in the technical report [10]. The three components of the rostrum, namely the soft cartilage, the hard cartilage, and the tissue are modeled using the material properties of steel to focus attention on the geometry of the rostrum rather than the varying material properties for the initial validation of the methodology. The rostrum is formulated as a complex network flow model by extracting the node and connectivity information from the computational mechanics model. The weights of the network are obtained from the von Mises stresses in the output database file produced from the numerical experiments on rostrum. The information obtained from the numerical experiments is fed to the maximum flow algorithm described in [12]. The source and sink are identified and specified in the data input to the maximum flow/minimum cut algorithm.

Figure 2 (a) shows the results obtained from the maximum flow/minimum cut algorithm. The red region demonstrates the formation of force chains in the rostrum. At a uniform pressure of 1.428 MPa, the force chains are formed in the lower left region of the rostrum. This behavior is may be attributed to the unsymmetrical geometry of the rostrum. As the uniform pressure increases to 2.857 MPa, the force chains start forming in the lower right region of the rostrum. At 4.235 MPa, stress localization regions are seen near the center bone indicative of the structure being under tension. The force chains are populated in the bottom part of the rostrum that is attached to the mouth of the fish. Since the rostrum is thicker near the mouth of the fish, it is able to withstand larger loads as compared to the upper, thin region. Figure 2(b) shows the von Mises stresses on the rostrum at a uniform pressure of 27.5 MPa and flow network analysis at 7.173 MPa. It is clear that the maximum flow/minimum cut algorithm is able to predict the tension and yielding region much earlier i.e., at a uniform pressure of 7.143 MPa as compared to the

numerical experiments that show yielding in that region at a uniform pressure of 27.5 MPa as depicted in Figure 2(b).

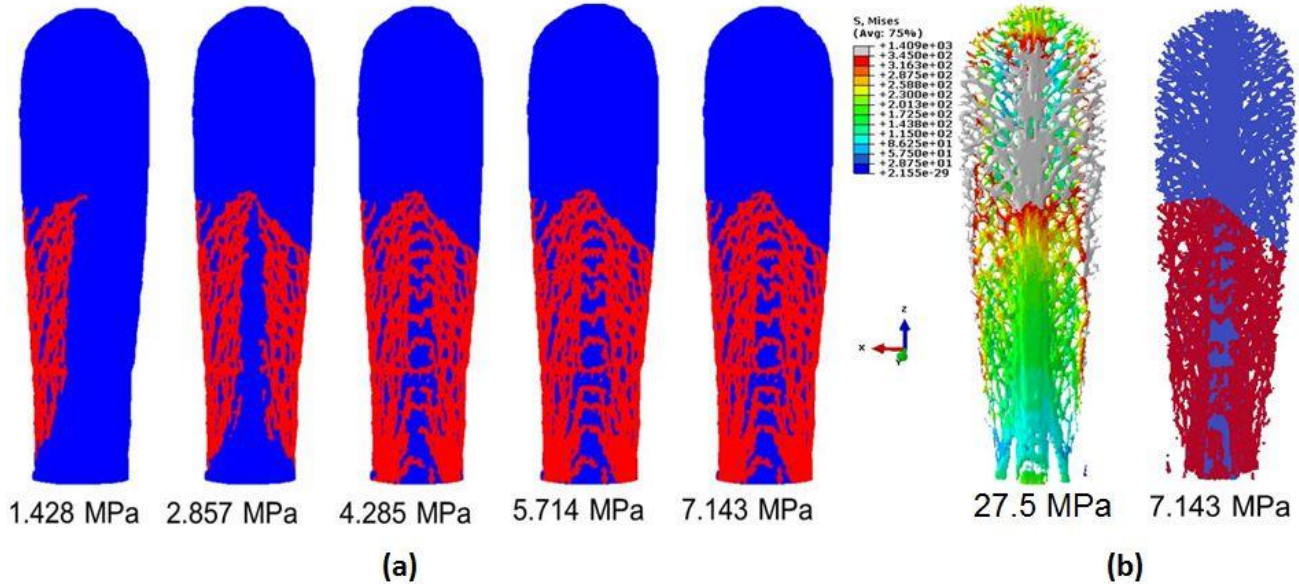


Figure 2: (a) Network flow analysis of load distribution with increasing pressure on rostrum's bottom surface with increasing pressures from 1.428 MPa to 7.143 MPa (b) Computational mechanics experiment showing yielding of hard cartilage of rostrum under uniform pressure of 27.5 MPa and network flow analysis showing the load distribution at 7.143 MPa.

CONCLUSIONS

This study has successfully utilized advanced mathematical algorithms to gain insight into the underlying kinematics associated with formation of force chains when a hierarchical biostructure is subjected to uniform pressure loading condition. A flow network approach was used for the analysis of the indeterminate lattice architecture. The flow network was able to identify strain localization in the tensile region of the rostrum. Moreover, the asymmetrical response of the rostrum to uniform loading was highlighted through the force chain formation. Also, flow network was able to identify the yielding region of the rostrum much earlier than the numerical experiments.

ACKNOWLEDGMENTS

The authors acknowledge the financial support provided by the U.S Army Engineer Research and Development Center (ERDC) Military Engineering 6.1 Basic Research program. Contributions made by Mississippi State University are greatly appreciated. The authors sincerely thank Dr. John Peters (MSU/ERDC) and Dr. Antoinette Tordesillas (University of Melbourne) for discussions and guidance regarding the topic.

LITERATURE CITED

- [1] V. Lefort, G. Pijaudier, D. Gregoire, "Analysis by ripley's function of the correlations involved during failure in quasi-brittle materials: experimental and numerical investigations at the mesoscale," *Engineering Fracture Mechanics*, 2015.

- [2] A. Tordesillas, D. M. Walker, G. Froyland, J. Zhang, R. P. Behringer, "Transition dynamics and magic-number-like behavior of frictional granular clusters," *Physical Review E*, vol. 86, no. 011306, 2012.
- [3] G. Riveros, R. Patel, J. Hoover, "Swimming enhancement induced by the rostrum of the paddlefish (polyodon spathula) in laminar flows: A multiphysics, fluid-structure interaction analysis," *Applied Mathematical modelling*, In Review.
- [4] R. Patel and G. Riveros, "Towards development of innovative bioinspired materials by analyzing the hydrodynamic properties of polyodon spathula (paddlefish) rostrum," ERDC/ITL TR-13-4.
- [5] J. B. Allen and G. A. Riveros, "Hydrodynamic characterization of the polyodon spathula rostrum using cfd," *Journal of Applied Mathematics*, 2013.
- [6] G. Riveros, R. Patel, J. Hoover, "Swimming and energy dissipation enhancement induced by the rostrum of paddlefish (polyodon spathula): A multiphysics, fluid-structure interaction analysis," in *Materials Research Society Fall Meeting*, Boston, 2014.
- [7] R. K. Ahuja, T. L. Magnanti, J. B. Orlin., "Network Flows: Theory, Algorithms, and Applications.," in *Proceedings of the National Academy of Sciences, 1st Edition*, 1993.
- [8] M. E. J. Newman, "Networks: An Introduction," Oxford University Press, Oxford , 2010.
- [9] R. R. Patel, G. A. Riveros, F. J. Acosta, E. J. Perkins, J. J. Hoover, D. S. Thompson, "Early detection of failure mechanisms in resilient bio-structures: A complex network study," ERDC-TR, In Review.
- [10] F. J. Acosta, G. A. Riveros, R. Patel, W. Hodo, "Numerical simulation of biological structures:Paddlefish Rostrum," ERDC TR, In review.
- [11] Hibbit, Karlsson, Sorenson, Inc., Abaqus/Standard User's Manual, Vol. I & II, Pawtucket, Rhode Island, 1994.
- [12] K olmogorov, Y. Boykov, Vladimir, "An Experimental Comparison of Min-Cut/Max-Flow Algorithms for Energy Minimization in Vision," in *In IEEE Transactions on Pattern Analysis and Machine Intelligence (PAMI)*, 200

A Study of Large-Scale Surface Fluxes, Processes and Heavy Precipitation Associated with Land Falling Tropical Storm Lee over Gulf of Mexico using Remote Sensing and Satellite Data

Warith Abdullah, Remata Reddy, Ezat Heydari and Wilbur Walters Jackson
State University, Jackson, Mississippi 39217

Corresponding Author: Warith Abdullah, email: nullexponent@gmail.com

ABSTRACT

Tropical Storm (TS) Lee formed September 2nd, 2011 from a broad but disorganized tropical wave that entered Western Caribbean in late August. While the storm's core meandered inland on September 4 roughly 50 miles (80 km) southwest of Lafayette, LA, squalls impacted Gulf Coast the day prior. On September 4th, TS Lee's pressure drops to 986 mb and made landfall on Louisiana-Mississippi coast on September 5th. Lee's high moisture content and slow movement promoted 24 hour rainfall totals in excess of 5 inches (127 mm) to 11 inches (281 mm) in most locations over the Gulf States. Despite lacking wind/pressure intensity, TS Lee absorbed large amounts of moisture, contributing to intense precipitation. We further investigated possible relationships between large-scale heat fluxes and intensity changes associated with landfall of TS Lee, and examined vertical motions associated with intensity change of T.S. Data on Convective Available Potential Energy (CAPE), sea level pressure and wind speed were obtained from Atmospheric Soundings and NOAA National Hurricane Center (NHC), respectively for the period of August 25 to September 10, 2011. We developed an empirical model and C++ program to calculate surface potential temperatures and heat fluxes using above data. Vertical motions were computed using CAPE values. Studies showed large-scale heat fluxes reached maximum (4500 W m^{-2}) with central pressure 986 mb. CAPE and vertical motions peaked during landfall. Large vertical atmospheric motions associated with land falling Tropical Storm Lee produced severe weather including thunderstorms, tornadoes and large-scale floods associated with heavy precipitation.

Keywords: Tropical Storm, Remote Sensing, Storm Intensification

INTRODUCTION

A tropical cyclone (synonymous with hurricane) is an intense, low-level atmospheric warm-core vortex that originates over tropical oceans and is energetically driven principally by latent heat of evaporation from the ocean surface. Tropical cyclones are devastating natural disasters especially at the time of landfall. A tropical cyclone's sustained high winds, torrential rainfall and storm surge dramatically impact and alter coastal habitats, coastlines, man-made structures and cause loss of life. Over the decades, global research to forecast tropical cyclones through numerical simulation has grown. Now, spanning Global Circulation Models (GCM's), ensemble models such as ECMWF, NOGAPS, UKMET, GFDL and many others, has led to increased understanding of tropical

cyclone behavior. However, many uncertainties exist particularly in terms of cyclogenesis, intensification potential and the prediction of both processes. One parameter of increasing interest for tropical cyclone intensification investigation is the ocean-atmosphere interface (OAI). At the state of current modeling techniques, the OAI is poorly understood and thus poorly represented in model simulations¹⁰.

Limitations exist for reliable metrics to capture the amount of latent energy per unit area (e.g., satellite data correction, insufficient buoy coverage etc.) in addition to computing reliable approximations of energy conversion-transfer values during any given tropical cyclone. We choose a case study, tropical storm Lee in the domain of the Gulf of Mexico, to examine fundamental parameters associated with tropical

cyclone energy processes and surface fluxes with respect to the OIA. The following descriptive background was used as foundational criteria in our investigation of tropical storm Lee.

Tropical cyclone development

Regions and conditions. Each year on average, eleven tropical storms (of which six become tropical cyclones) develop over the Atlantic Ocean, Caribbean Sea, or Gulf of Mexico. The tropical cyclone season is generally during June-November and the 2011 season recorded 19 named systems¹. Tropical cyclones usually develop between 5° to 30° north and south of latitudes-- a region characterized by warm ocean waters with sea surface temperatures (SST) exceeding 26° C, as well as sufficient Coriolis acceleration. Energy is transferred to the storm via evaporation, where water vapor condenses and releases enormous amounts of latent heat to drive intensification. A mature tropical cyclone is structured of individual convective cells comprising regions of rising and sinking air parcels associated with small scale cumulus convection². This convective activity produces intense thunderstorms that organize into clearly defined spiral bands.

Convective Available Potential Energy (CAPE). CAPE is a metric used to forecast large scale disturbances leading to severe weather¹. CAPE is computed as the amount of buoyant energy available to accelerate an air parcel vertically, with maximum vertical speed estimates in units of Joules per kilogram ($J\ kg^{-1}$). A higher CAPE value represents increasingly unstable atmospheric conditions to fuel storm growth and intensification. Although the current study focuses on CAPE values for intensification rates, CAPE values can be analyzed for pre-land fall effects of storm systems and contribute to early warning forecasts through predictive analysis².

Vertical motions. The uplift mechanism during energy transfer can be expressed in vertical wind velocities between the OAI. Associated velocities greater than $50\ m\ s^{-1}$ are observed during severe storm activity³.

Precipitation. Tropical cyclones produce staggering amounts of rainfall, with maximum rates meeting or exceeding meters per day especially near the eyewall and when the storm becomes extra-tropical³. For this case study, we observe precipitation rates and total amounts as

a function of CAPE energy and precipitable water content due to the energy transfer rate through the OAI.

Tropical cyclone mitigating processes

Mechanisms and features. Atmospheric and topographic processes and features can prohibit tropical cyclone development and intensification. Among those include (i) vertical wind shear, (ii) dry air intrusion, (iii) topographical obstructions (i.e., land masses and/or mountain ranges), (iv) sea surface temperatures less than 26° C⁸ and (v) cold-water upwelling. We focus on parameters that impact the OIA: vertical wind shear, dry air intrusion and topography.

Vertical wind shear. Vertical wind shear is defined as the amount of change in wind direction and velocity with increasing altitude⁵. As wind speed increases with height, thunderstorms within a tropical cyclone become vertically slanted downwind and latent heat released by condensation is distributed over a larger area. Depending on wind shear magnitude and intensity, either a reduction or negation of intensification potential for tropical cyclone development will occur.

Dry air intrusion. Tropical cyclones require a constant supply of warm, moist air to support and sustain their powerful convective processes. The influx of dry air is extremely disruptive as it suppresses necessary convective uplift. Dry air infiltrates a storm, dispels latent heat through absorption and increases atmospheric stability.

Topography. Topography is considered when a tropical cyclone develops nearby, or passes over landmass during its track², cutting the storm off from the ocean-surface and disrupting the OIA. Topography type impacts tropical cyclones differently: 1) flat terrain will disrupt energy supply and 2) elevated, rugged terrain may disrupt storm structure altogether. Interestingly, the increased frictional force over land acts to decrease maximum sustained winds and also increase gusts felt at the surface, though these effects are most prominent with mountain ranges⁹.

Case Study

Tropical storm Lee. Tropical storm Lee formed on September 2nd from a broad but disorganized tropical wave that entered the Western Caribbean in late August. The main center of circulation

meandered inland on September 4th roughly 50 miles (80 km) southwest of Lafayette, LA and the squalls impacted the Gulf Coast as early as September 3rd. Tropical storm Lee's high moisture content and slow velocity promoted 24-hour rainfall totals in excess of 5 inches (127 mm) in most locations, including New Orleans Airport and Holden, LA where 11.05 inches (281 mm) and 15.43 inches (393 mm) fell, respectively⁶. Tropical storm Lee became post-tropical on September 5th, its remnants moving northeast to drench regions along the axis of the Appalachian Mountain range. Several locations set new 24-hour rainfall records; of noteworthy mention was Jackson, MS where 11.68 inches (297 mm) exceeding the previous record of 8.54 inches (217 mm) set in 1979; and Chattanooga, TN received 9.85 inches (250 mm), exceeding the previous 7.61 inches (193 mm) record set in 1886. Tropical storm Lee caused 21 fatalities, over 250 million USD in damages and spawned EF-0 and EF-1 tornadoes totaling 40 reports⁶.

METHODS AND ANALYSIS

In the present study, we utilized satellite and remote sensing products to investigate the OAI components with respect to tropical storm Lee.

Remote Sensing products

GOES-8. To ascertain tropical storm Lee's geospatial domain, as well as its structure, we used visible-imagery from GOES-8 satellite instrument channels 1 through 5 (Figure 1).



Figure 1. GOES-8 visible satellite image of T.S. Lee.

GOES-13 East. We used GOES-13 East infrared (IR) cloud-top temperature remapped imagery (Figure 2) to investigate storm intensities, precipitation potential.

Image spatial resolution is 4km, displayed at a Mercator projection and captured at $\sim 11 \mu\text{m}$ ³. GOES-13 East Geostationary Water Vapor imagery (Figure 3) was used to investigate low and relative upper-level moisture content and advection, regions of environmental forcing and dry- air content. Water vapor imagery was captured with a spectral weight near $6.7 \mu\text{m}$ and displayed at 16km spatial resolution and Mercator projection⁴.

Advanced Microwave Sounding Unit (AMSU).

Wind shear (Figures 4 and 5), wind velocity (Figure 6) and minimal central pressure (Figure 7) were investigated using NHC best-track analysis and AMSU intensity estimates from the Cooperative Institute for Meteorological Satellite Studies. The Knaff-Zehr-Courtney (KZC P-W) values were obtained by applying the KZC P-W pressure-wind relationship to the best-track wind data. Estimates during the extra-tropical stage are partially based on analyses from the NOAA Hydrometeorological Prediction Center (HPC). Dashed vertical lines correspond to 0000 UTC and the solid vertical line corresponds to the time of landfall.⁵ Aircraft observations have been adjusted for elevation using 90%, 80%, and 80% adjustment factors for observations from 700 mb, 850 mb, and 1500 ft, respectively⁵.

Naval Coupled Ocean Data Assimilation system

(NCODA). Daily Oceanic Heat Content (OHC) estimates (Figure 8) were obtained to investigate available energy in degrees Kelvin. OHC has been provided by J. Cummings of the Naval Research Lab and is calculated from fields generated by the Naval Coupled Ocean Data Assimilation system (NCODA; Cummings 2005)⁷. The spatial grid spacing is 0.2 Latitude x 0.2 Longitude and the units of the estimates are given as kJ cm^{-2} .

Atmospheric Sounding products. Atmospheric Soundings were obtained from the University of Wyoming to investigate environmental instability during tropical storm Lee. The SKEW-T diagram from Slidell, LA station (Figure 9), though the only reliable measurement during tropical storm Lee, provided an index for instability. Height (in millibars and meters) is defined on y-axis and temperature (in degrees Celsius) on the x-axis. The thick black line to the right represents the environmental lapse rate (ELR); the thick black line to the left represents dew point and the thin black line to right of ELR is the Theoretical Air Parcel Plot (TAPP).

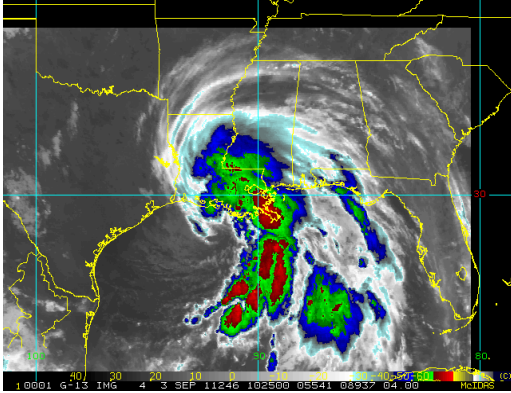


Figure 2. GOES-13 Enhanced IR Imagery for Tropical Storm Lee, September 03, 2011

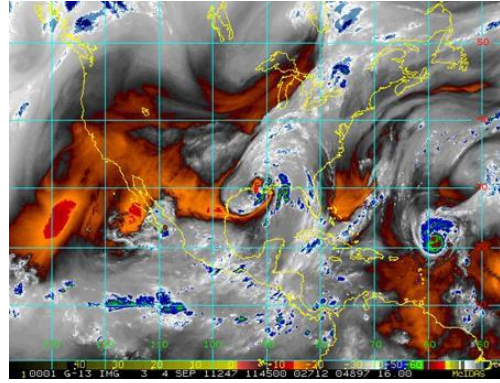


Figure 3. GOES-13 16 km Geostationary Water Vapory Imagery for Tropical Storm Lee, September 04, 2011

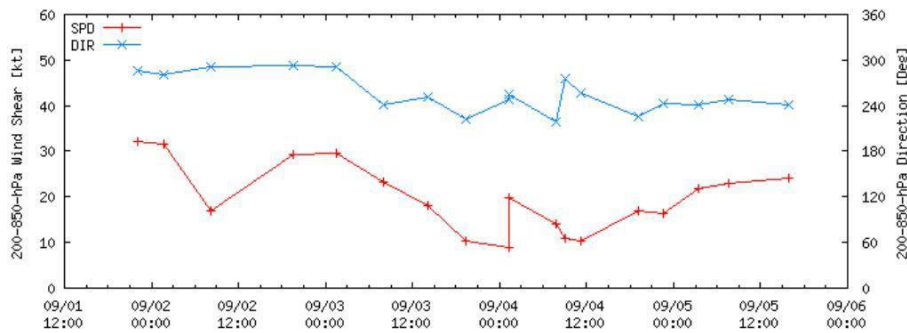


Figure 4. AMSU Area- Averaged Wind Shears and Layer Means at 250-800 hPa height for Tropical Storm Lee, 2-5 September 2011. Red horizontal-line corresponds to wind speed (kt), blue horizontal-line corresponds to wind direction (degrees).

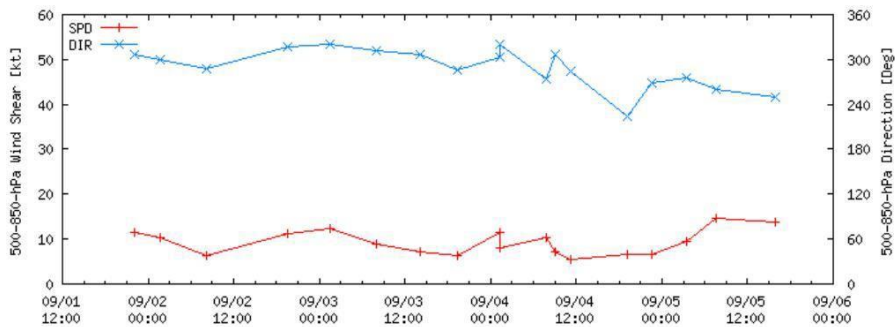
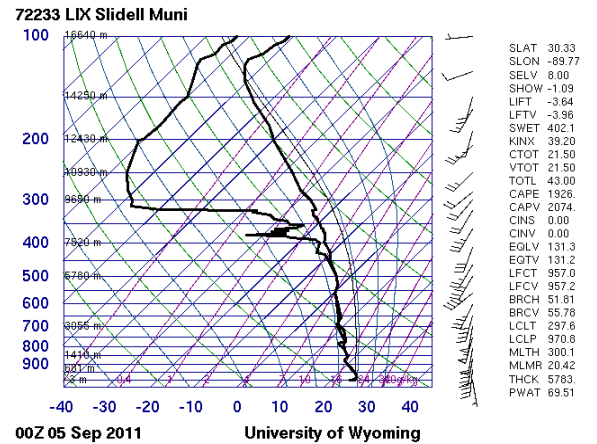
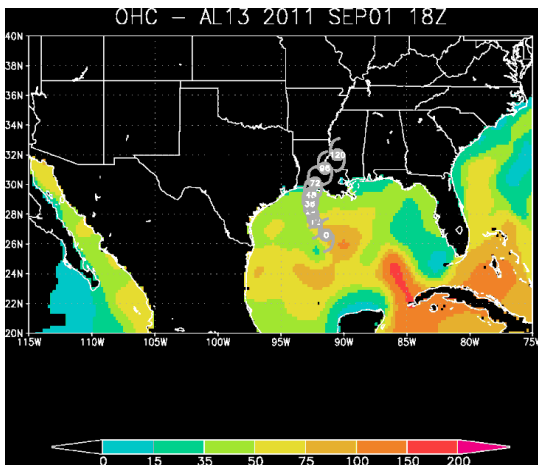
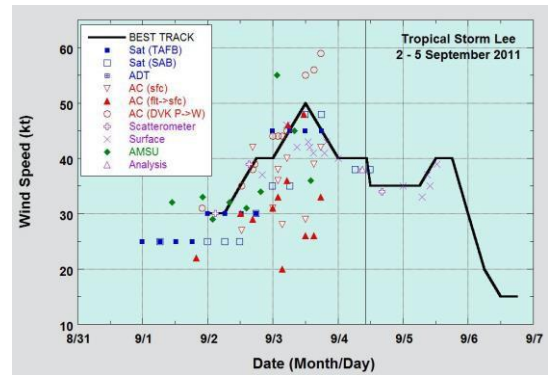
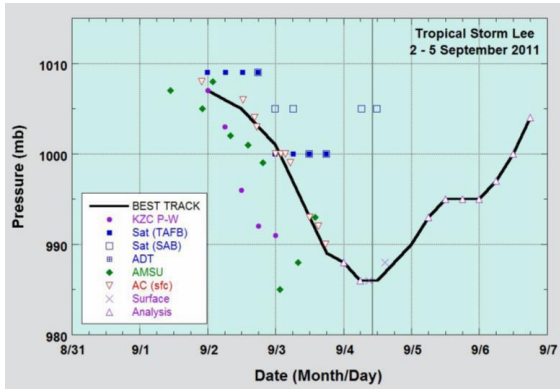


Figure 5. AMSU Area- Averaged Wind Shears and Layer Means at 500-800 hPa for Tropical Storm Lee, 2-5 September 2011.



Computations

We derived computations for CAPE using an empirical model and C++ algorithm. CAPE provides a measure of the maximum possible kinetic energy that a statically unstable air parcel can acquire.

Therefore, it provides a guide to the strength of convection and instability in the atmosphere. Vertical velocity is calculated from CAPE at the Equilibrium Level (EL). The vertical velocity of an air parcel by buoyancy is given by:

$$\frac{Dw}{Dt} = g \frac{T_{parcel} - T_{env}}{T_{env}} \quad (\text{eq. 1})$$

Where w is the vertical velocity, T_{parcel} is the temperature of the air parcel, T_{env} is the temperature of the environment and g is the acceleration due to gravity.

CAPE can be computed as:

$$\int_{LFC}^{EL} g \left[\frac{T_{parcel} - T_{env}}{T_{env}} \right] Dz \quad (\text{eq. 2})$$

We want an expression for computing the maximum vertical atmospheric velocity at the EL, w_{max} . It can now be derived based upon CAPE. Note that the expression $\frac{Dw}{Dt}$ in equation 1 can be written as:

$$\left(\frac{Dw}{Dt} \right) = \left(\frac{Dw}{Dz} \right) \times \left(\frac{Dz}{Dt} \right) \quad (\text{eq. 3})$$

Since $\frac{Dz}{Dt} = w$,

$$\frac{Dw}{Dt} = w \frac{Dw}{Dz} \quad (\text{eq. 4})$$

If equation 4 is integrated vertically from the Level of Free Convection (LFC) to the EL following the motion of the parcel, the result is:

$$\frac{w^2}{2} = \int_{LFC}^{EL} g \left(\frac{T_{parcel} - T_{env}}{T_{env}} \right) Dz \quad (\text{eq. 5})$$

Note that the right hand side of equation 5 is just the definition of CAPE. Therefore, the expression for w_{max} is

$$w_{max} = \sqrt{2CAPE} \quad (\text{eq. 6})$$

RESULTS AND DISCUSSION

Tropical storm Lee covered a generous area over the Gulf of Mexico. Available OHC ranging > 100 K, sea surface temperatures between 29° and 31° C, and lack of upper-level prevailing winds granted a favorable OAI environment for tropical storm Lee to develop and sequester large amounts of energy as CAPE values exceeded 1000 J kg⁻¹, peaking at 2045 J kg⁻¹ on September 4th. On average, CAPE values for severe storms are approximately 2300-3000 J kg⁻¹. Thus, the CAPE values computed during tropical storm Lee translated to only moderate atmospheric instability, as shown from 175-850 mb atmospheric sounding height analysis at Slidell, LA. GOES-13 East IR imagery shows modestly organized and significant convective activity predominantly within tropical storm Lee's ESE and WNW quadrants.

Tropical storm Lee reached its lowest central pressure of 986 mb and its peak vertical velocity of 63.95 m s⁻¹ on September 4th, coinciding with its peak CAPE. However, 250-800 hPa vertical layer analysis shows persistent WNW shear between approximately 11 and 33 knots from the period September 2nd through 5th. In addition, GOES-13 East water vapor imagery shows prominent dry-air intrusion within the WSW quadrant of the storm, disrupting the OAI energy exchange. Tropical storm Lee reached its 50 knot peak wind velocity on September 3rd, despite a 1024 J kg⁻¹ CAPE value. Tropical storm Lee obtained large quantities of moisture that contributed to the intense precipitation event upon the Gulf Coast region with maximum rainfall totals of 15.48" in Holden, LA, 13.55"

in Florence, MS and 12.62" in Mobile, AL.

CONCLUSIONS

Strong vertical motions and OAI associated with moderate amounts of instability coupled with consistent CAPE values allowed tropical storm Lee to absorb massive amounts moisture, contributing to Intense precipitation. Moderate wind shear and a prominent dry-air intrusion prevented tropical storm Lee from intensifying further. Though these processes typically negatively affect tropical cyclone intensification, tropical storm Lee was impacted by an unusually powerful blocking high-pressure system positioned in the interior Midwest of the United States. We surmise the intensity of the dry air, as opposed to the presence of wind shear, played a greater role in mitigating intensification through disruption of the OAI. Interestingly, CAPE, vertical motions and central pressure peaked shortly after landfall. This behavior is unusual, as tropical cyclones typically lose energy exchange from the OAI by crossing over topography. We hypothesize this may exhibit a delayed energy conversion from latent heat to mechanical energy, however the energetic dynamics warrant further study especially with respect to OAI behavior. It is our goal to extend this case study with several more studies and develop a greater platform towards understanding the OAI.

ACKNOWLEDGEMENTS

This work was supported by NASA/NICE grant NNX10AB49A.

LITERATURE CITED

1. Emanuel, K.A., 1986: An Air-Sea Interaction Theory for Tropical Cyclones, *J. Atmos. Sci.*, 45, 1143-1155
2. Holton, James R. An Introduction to Dynamic Meteorology, 4th Edition. Academic Press Inc., San Diego, 1992, pp 370
3. Kantave Greene, Lail Hossain and Remata Reddy, A Study of Vertical Motion and Associated Thunderstorm Activity over the West Coast of Gulf of Mexico, NCUR 99 Proceedings, pp 1294-1298.
4. Cooperative Institute for Meteorological Satellite

- Studies (CIMSS) Tropical Cyclones
<http://tropic.ssec.wisc.edu/tropic.php>
 [Accessed 3-8-2012] NOAA Satellites and
 Information; National Environmental
 Satellite, Data and Information Service;
 Regional and Mesoscale Meteorology Branch
 (RAMMB)
<http://rammb.cira.colostate.edu/products/tc-realtime> [Accessed 4-16-2012]
5. NOAA, National Weather Service (NWS) National
 Hurricane Center (NHC)
<http://www.nhc.noaa.gov/pastall.shtml>
 [Accessed 5-23-2012]
6. UWYO, University of Wyoming Department of
 Atmospheric Science
<http://weather.uwyo.edu/upperair/soundin>
[g.html](#) [Accessed 4-16-2012]
7. Peng, M.S., Fu, B., Li, T., and Stevens, D.E., 2012:
 Developing versus Nondeveloping
 Disturbances for Tropical Cyclone Formation.
 Part I: North Atlantic. *Mon. Wea. Rev.*, **140**
 1047- 1066
8. Chang, S. W.J., 1982: The Orographic Effects
 Induced by an Island Mountain Range on
 Propagating Tropical Cyclones. *Mon. Wea.*
Rev., **Vol 110** 1255 – 1270
9. Tallapragada, V., et al 2014: Hurricane Weather
 Research and Forecast (HWRF) Model 2014
 Scientific Documentation. *NOAA/NWS/NCEP*

82ND ANNUAL MEETING

THAD COCHRAN CONVENTION CENTER
HATTIESBURG, MS

FEBRUARY 23-24, 2017

**SUBMIT ABSTRACTS BY
NOV. 15, 2017**

Make sure to Renew Your Membership

Can also be done on-line at : <http://msacad.org/>

Membership/Registration opens December 1, 2017

Renew and join early to avoid late fees

MISSISSIPPI ACADEMY OF SCIENCES ABSTRACT FORM/MEMBERSHIP FORM

ABSTRACT INFORMATION

Abstract title: _____

Name of Presenting Author(s): _____

If you are a student please fill-out the next line

Name of Mentor and e-mail of Mentor _____

(Presenter must be current (i.e., 2016 membership dues must be paid), student member, regular member or life member of the MAS)

Telephone _____ Email _____

Check the division in which you are presenting

- ___ Agriculture and Plant Science ___ Health Sciences ___ Physics and Engineering
___ Cellular, Molecular, and Dev. Biol ___ History and Philosophy of Sciences ___ Psychology and Social Sciences
___ Chemistry and Chem. Engineering ___ Math., Computer Sci and Statistics ___ Science Education
___ Ecology and Evolutionary Biology ___ Marine and Atmospheric Sciences ___ Zoology and Entomology
___ Geology and Geography

Complete either the Membership/Pre-Registration form if you plan to attend and present at the meeting if you do not plan to attend the meeting please complete the membership form

MEMBERSHIP/ PRE-REGISTRATION INFORMATION

New ___ Renewal ___

Mr. Ms. Dr. _____

Address _____

City, State, Zip _____

School or Firm _____

Telephone _____ Email _____

PLEASE INDICATE DIVISION YOU WISH TO BE AFFILIATED _____

Before January 15, 2018.....Regular Member/Pre-Registraion \$130 Student Member/ Pre-registration \$50

After January 15, 2018.....Regular Member/Registraion \$170 Student Member/ Pre-registration \$60

MEMBERSHIP INFORMATION

New ___ Renewal ___

Mr. Ms. Dr. _____

Address _____

City, State, Zip _____

School or Firm _____

Telephone _____ Email _____

PLEASE INDICATE DIVISION YOU WISH TO BE AFFILIATED _____

Regular Member \$30 Student Member \$10 Life Member \$450
Educational Member \$550 Corporate Patron \$1000 Corporate Donor \$500

CHECKLIST

Please complete the following:

- ___ Enclose title of abstract (even if abstract has been submitted electronically)
___ Complete membership/registration form (this form)
___ Enclose the following payments (Make checks payable to Mississippi Academy of Sciences)
___ \$25 per abstract
___ \$130 regular membership/pre-registration fee OR \$50 student membership/pre-registration fee
___ You must supply a check # _____ or P.O. # _____ (or indicate Pay Pal confirmation) _____

MISSISSIPPI ACADEMY OF SCIENCES—ABSTRACT INSTRUCTIONS
PLEASE READ ALL INSTRUCTIONS BEFORE YOU SUBMIT YOUR ABSTRACT ON-LINE

- Your paper may be presented orally or as a poster. Oral presentations are generally 15 minutes. The speaker should limit the presentation to 10-12 minutes to allow time for discussion; longer presentations should be limited accordingly. Instructions for [poster presentations](#) are linked here.
- Enclose a personal check, money order, institutional check, or purchase order for \$25 publication charge for each abstract to be published, payable to the Mississippi Academy of Sciences. The publication charge will be refunded if the abstract is not accepted.
- The presenting author must be a member of the Academy at the time the paper/poster is presented. Payment for membership of one author must be sent for the abstract to be accepted.
- Attendance and participation at all sessions requires payment of registration.
- Note that three separate fees are associated with submitting and presenting a paper at the annual meeting of the Mississippi Academy of Sciences.
 1. An abstract fee is assessed to defray the cost of publishing abstracts and
 2. A membership fee is assessed to defray the costs of running the Academy.
 3. Membership/Preregistration payment (\$130 regular; \$50 student) may accompany the abstract, or you may elect to pay this fee before January 15th, or pay full late membership/registration fees at the meeting (\$170 regular, \$60 student).
- Abstracts may **only** be submitted on line via a link through the MAS website. The appropriate abstract fees can be paid via Paypal or sent via mail to Barbara Holmes at the Academy address.
- **Late abstracts will be accepted with a \$10 late fee during November increased to \$25 after that. Late abstracts will be accepted only if there is room in the appropriate division. They will be published in the April issue of the MAS JOURNAL.**
- Submit your appropriate fees **NO LATER THAN January 15th, 2017.**

Ms. Gerri Wilson
Mississippi Academy of Sciences
Post Office Box 55907
Jackson, MS 39296-5907

GUIDELINES FOR POSTER PRESENTATIONS

- The Academy provides poster backboards. Each backboard is 34" high by 5' wide. Mount the poster on the board assigned to you by your Division Chairperson. Please do not draw, write, or use adhesive material on the boards. You must provide your own thumb tacks.
- Lettering for your poster title should be at least 1" high and follow the format for your abstract. Lettering for your poster text should be at least 3/8" high.
- Posters should be on display during the entire day during which their divisional poster session is scheduled. They must be removed at the end of that day.
- Authors must be present with their poster to discuss their work at the time indicated in the program.

Author Guidelines

Editorial Policy. The Editorial Board publishes articles on all aspects of science that are of general interest to the scientific community. General articles include short reviews of general interest, reports of recent advances in a particular area of science, current events of interest to researchers and science educators, etc. Research papers of sufficiently broad scope to be of interest to most Academy members are also considered. Articles of particular interest in Mississippi are especially encouraged.

Research papers are reports of original research. Submission of a manuscript implies that the paper has not been published and is currently at the time of submission being considered for publication elsewhere. At least one of the authors must be a member of the Academy, and all authors are encouraged to join.

Manuscripts. Submit the manuscript electronically to the Mississippi Academy of Sciences under your profile in the member location of the website. Please also provide a cover letter to the Editor of the Journal. The cover letter should authorize publication: give the full names, contact information, for all authors; and indicate to whom the proofs and correspondence should be sent. Please notify the Editor on any changes prior to publication.

Manuscripts must adhere to the following format:

- One inch margins on 8.5 x 11 inch paper;
- Text should be left-justified using twelve point type;
- Double spaced throughout, including the title and abstract;
- Arabic numerals should be used in preference to words when the number designates anything that can be counted or measured (7 samples, 43 species) with 2 exceptions:
- To begin a sentence (Twenty-one species were found in...)
- When 2 numeric expressions are adjacent in a sentence. The number easiest to express in words should be spelled out and the other left in numeric form (The sections were divided into eight 4-acre plots.).
- Measurements and physical symbols or units shall follow the International System of Units (SI *Le Système international d'unités*) with metric units stated first, optionally followed by United States units in parentheses. *E.g.:* xx grams (xx ounces); and
- Avoid personal pronouns.

Format

Abstract. In 250 or fewer words summarize any new methods or procedures critical to the results of the study and state the results and conclusions.

Introduction. Describe the knowledge and literature that gave rise to the question examined by, or the hypothesis posed for the research.

Materials and methods. This section should describe the research design, the methods and materials used in the research (subjects, their selection, equipment, laboratory or field procedures), and how the findings were analyzed.

Results. The text of the results should be a descriptive narrative of the main findings, of the reported study. This section should not list tabulated data in text form. Reference to tables and figures included in this section should be made parenthetically in the text.

Discussion. In this section compare and contrast the data collected in the study with that previously reported in the literature. Unless there are specific reasons to combine the two, as explained by the author in the letter of transmittal, Results and Discussion should be two separate sections.

Acknowledgments. Colleagues and/or sources of financial support to whom thanks are due for assistance rendered in completion of the research or preparation of the manuscript should be recognized in this section rather than in the body of the text.

Literature cited. List references alphabetically. Cite references in the text by author and year of publication (e.g., Smith, 1975; Black and Benghuzzi, 2011; Smith et al., 2010; Smith, 2011a, 2011b). The following examples illustrate the style to be used in the literature list.

Black DA, Lindley S, Tucci M, Lawyer T, Benghuzzi H. A new model for the repair of the Achilles tendon in the rat. *J Invest Surg.* 2011; 24(5): 217-221.

Pearson HA, Sahukhal GS, **Elasri** MO, Urban MW. Phage-bacterium war on polymeric surfaces: can surface-anchored bacteriophages eliminate microbial infections? *Biomacromolecules.* 2013 May 13;14(5):1257-61.

Bold, H.C., C.J. Alexopoulos, and T. Delevoryas. 1980. *Morphology of plants and fungi*, 4th ed. Harper and Row, New York. 819 pp

Web-page

- name of author(s) -if known
- title of the work - in quotes, if known
- title of the Web page - in italics, if applicable
- date of last revision
- URL
- Date accessed

Example:

Ackermann, Ernest. "Writing Your Own Web Pages." *Creating Web Pages*. 23 Oct. 1996.
<http://people.umw.edu/~ernie/writeweb/writeweb.html> 10 Feb. 1997.

File available by anonymous FTP

- name of author(s) -if known
- title of the work - in quotes, if known
- date of last revision
- URL
- Date accessed

Example:

American Civil Liberties Union. "Briefing paper Number 5, Drug Testing in the Work Place." 19 Nov. 1992. ftp://ftp.eff.org/pub/Privacy/Medical/aclu_drug_testing_workplace.faq
13 Feb. 1997.

Please Tables and Figures at the end of the manuscript submitted.

Tables. Tables must be typed double spaced, one table to a page, numbered consecutively, and placed at the end of the manuscript. Since tables must be individually typeset, consolidation of data into the smallest number of tables is encouraged. A horizontal double underline should be made beneath the title of the table, and single underlines should be made the width of the table below the column headings and at the bottom of the table. Do not use vertical lines, and do not place horizontal lines in the interior of the table. Use footnotes, to clarify possible questions within the table, should be noted by asterisks, daggers, or other symbols to avoid confusion with numerical data. Tables should be referred to parenthetically in the text, for example (Table 1).

Figures and illustrations. Figures may be photographs, computer -generated drawings, or graphs and should be placed at the end of the manuscript and referenced in the appropriate place.. All illustrations are referred to as "Figures" and must be numbered consecutively. Illustrations other than those generated by the author(s) must include permission for use and credit to the originator. Each figure must have a complete legend that is typed, double-spaced, on a separate sheet which precedes the figures in the manuscript. Figures should be referred to parenthetically in the text, for example (Fig. 1).

Footnotes. Text footnotes **should not be used**

Submission Preparation Checklist

As part of the submission process, authors are required to check off their submission's compliance with all of the following items, and submissions may be returned to authors that do not adhere to these guidelines.

1. The submission has not been previously published, nor is it before another journal for consideration (or an explanation has been provided in Comments to the Editor).
2. The text adheres to the stylistic and bibliographic requirements outlined in the Author Guidelines.
3. I acknowledge that if my manuscript is peer-reviewed and accepted for publication, there will be a paper charge fee of \$50/page for **non-Academy members**.
4. The manuscript file is in Microsoft Word format.

Copyright Notice

Authors who publish with this journal agree to the following terms:

1. Authors retain copyright and grant the journal right of first publication
2. Authors are able to enter into separate, additional contractual arrangements for the non-exclusive distribution of the journal's published version of the work (e.g., post it to an institutional repository or publish it in a book), with an acknowledgement of its initial publication in this journal.
3. Authors are permitted and encouraged to post their work online (e.g., in institutional repositories or on their website) prior to and during the submission process, as it can lead to productive exchanges, as well as earlier and greater citation of published